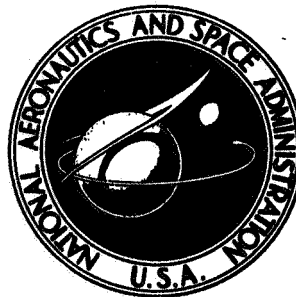


FINAL REPORT
RESEARCH IN THE DEVELOPMENT
OF AN
IMPROVED MULTIPLIER PHOTOTUBE

Contract NASw-1576

Prepared by

E. H. Eberhardt, F. H. Barr and P. R. Henkel
International Telephone and Telegraph Corporation
Industrial Laboratories Division
3700 East Pontiac Street
Fort Wayne, Indiana



National Aeronautics and Space Administration Headquarters
Washington, D. C. 20546

FACILITY FORM 502	N 68-35720	
	(ACCESSION NUMBER)	(THRU)
	78 (PAGES)	1 (CODE)
	CR-97079 (NASA CR OR TMX OR AD NUMBER)	09 (CATEGORY)



ITT Industrial Laboratories

*a division of International Telephone and Telegraph Corporation
3700 East Pontiac Street, Fort Wayne, Indiana 46803
Telephone (219) 743-7571 TWX 241-2065*

ITTIL 68-023

July 17, 1968

FINAL REPORT
RESEARCH IN THE DEVELOPMENT
OF AN
IMPROVED MULTIPLIER PHOTOTUBE

Contract NASw-1576

Prepared by

E. H. Eberhardt, F. H. Barr and P. R. Henkel

International Telephone and Telegraph Corporation
Industrial Laboratories Division
3700 East Pontiac Street
Fort Wayne, Indiana

Approved by

S. M. Johnson Jr., Manager
Advanced Product Development

M. F. Toohig, Manager
Tubes and Sensors Department

Dr. C. W. Steeg Jr., Director
Product Development

TABLE OF CONTENTS

		Page
1.0	TRIGGERED LIGHT SOURCE INVESTIGATIONS -----	1-1
2.0	AFTERPULSING INVESTIGATION -----	2-1
3.0	MATERIALS INVESTIGATION -----	3-1
3.1	Alkali Metals Used in Cathode Formation -----	3-1
3.2	Faceplate Materials -----	3-3
4.0	COUNTING EFFICIENCY -----	4-1
4.1	Light Source Calibration -----	4-1
5.0	SPECIAL MULTIPLIER TYPES -----	5-1
5.1	Fast Rise Time Multiplier -----	5-1
5.2	Windowless Multipliers -----	5-7
5.3	Multiplier Phototubes with Remotely Processed Cathodes -	5-12
6.0	ANALYSIS OF STANDARD ITTIL MULTIPLIER PHOTO- TUBE DATA -----	6-1
7.0	CORRELATION OF DARK CURRENT AND DARK COUNTING RATE -----	7-1

1.0 TRIGGERED LIGHT SOURCE INVESTIGATIONS

One of the most important problems in the investigation of the single electron counting properties of multiplier phototubes is the correlation (or possible correlation) of a given output charge pulse with a given input photon (i.e. a quantum of radiation). Ideally, perhaps, one would wish to introduce a single photon at a known time and then look for the presence or absence of a corresponding output pulse, the observed ratio of output pulses to input photons, averaged over many such observations, being the over-all effective detector quantum counting efficiency.

But control of this sort over the precise presence or absence of an input photon is, of course, impossible on a quantum uncertainty basis. Instead, Tusting, Kerns and Knudsen¹, in a classical quantum counting paper reduced the average intensity of the input flux to a level for which the probability of more than one photon was negligibly small. Then by gating their multichannel analyzer to observe only those MPT output pulses which corresponded, in time, to the triggered input flux (a few nanoseconds duration time), they were able to observe primarily only those output pulses corresponding to a single input photon. (They observed nothing, of course, for most of the observation time intervals.)

Probably the most surprising results of these experiments was the Poisson-type (peaked) output pulse height distribution which were obtained on all tubes tested. Previous to these tests, the consensus of opinion, based on non-triggered tube tests was that the distribution was exponential (i.e. non-peaked). Here, then, was a tool (triggered light source, gated analyzer) which might serve as a useful tool for investigating the counting properties of our own MPT's. In particular it might prove useful for:

- a. Investigating the source of the unexplained tail of the single electron distribution for small pulses, and
- b. Determining whether or not satellite (after-) pulsing is occurring.

To accomplish this was comparatively easy, since ITTIL has a suitable triggered fast light source (about 1 to 2 ns duration, 30 to 300 hz repetition rate) custom built for us by Edgerton, Germeshausen & Grier, Inc., which was in routine use for monitoring the transit time and transit time spread of our fast MPT's. Figure 1 shows a block diagram of the test configuration which was assembled, combining this fast triggered light source with our analyzing equipment.

1 R. F. Tusting, Q. A. Kerns, and H. K. Knudsen, "Photomultiplier Single-Electron Statistics," IRE Transactions on Nuclear Science, volume NS-9, number 3, pages 118-123; June 1963.

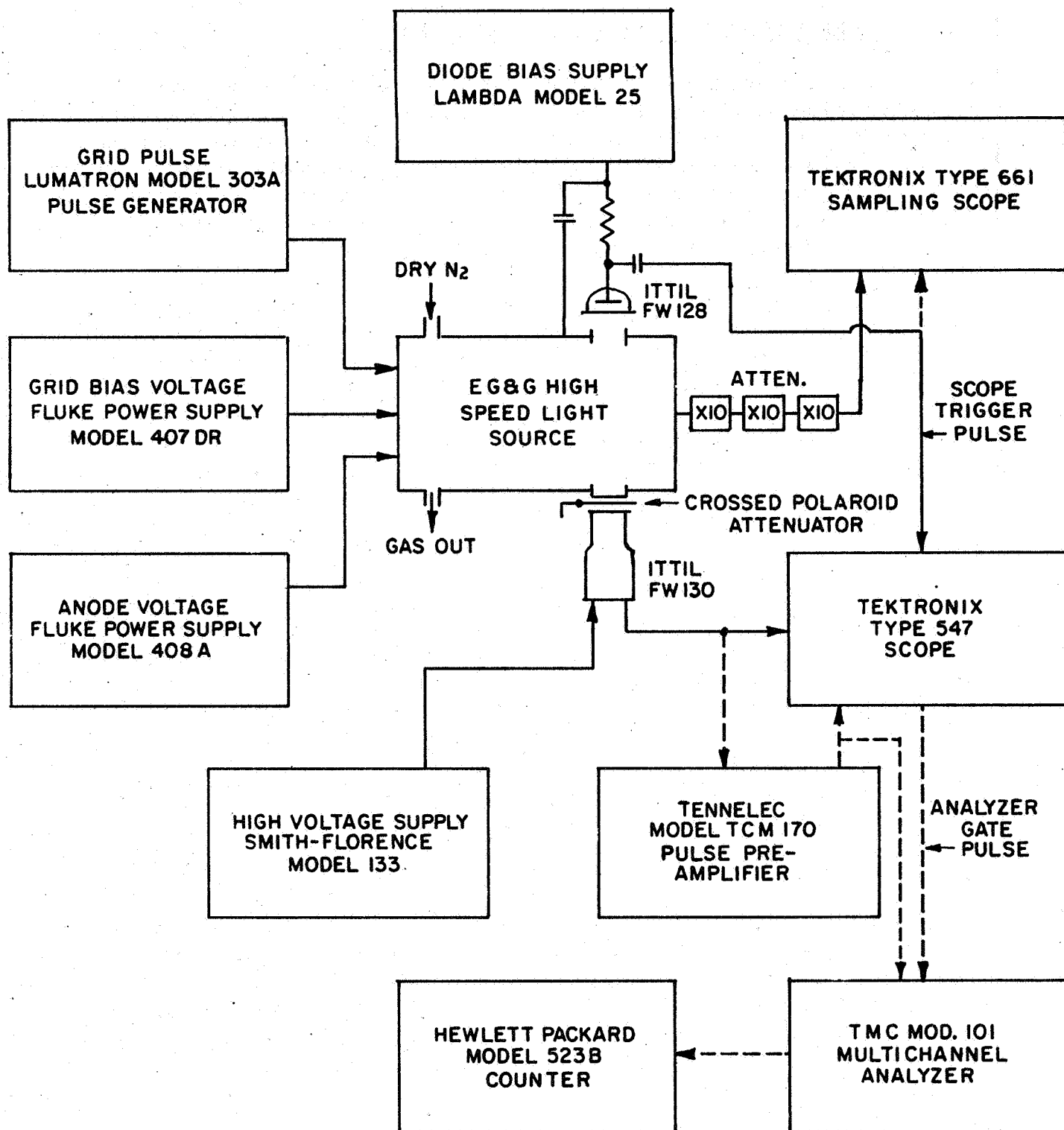


FIGURE 1.

The light source consists of a sealed enclosure, flushed with dry nitrogen, which contains a high frequency triode vacuum tube with the grid normally biased to cutoff. When the grid is pulsed on the tube conducts and discharges an R-C network in the cathode circuit producing an arc between a polished spherical electrode and a fine tungsten point, prepared in much the same manner as that used in field emission microscopy. The phototube under test sees the light through a pair of crossed polaroids for variable attenuation while the rise time of the light pulse is monitored by an ITTIL FW128 diode, which has a rise time that is short with respect to that of the light pulse. It should be mentioned, however, that this particular aspect of the equipment is not important for the work reported here, since the diode output is used only as a trigger pulse for the 547 oscilloscope. The sampling scope serves only to monitor the light and the diode cathode current pulse so that they may be adjusted for optimum amplitude and rise time.

The dashed lines indicate an alternate arrangement where by it was hoped to be able to gate the multichannel analyzer at some fixed time interval following a multi-electron pulse in order to determine if there was a definite time relationship between the multi- and single electron pulses. Matching output and input pulse requirements as well as obtaining the proper gating delay time, proved to be a problem with the equipment available and will require further effort in order to obtain the desired data.

Upon setting up this equipment it was soon discovered that each triggered multielectron output pulse (from many input photons in a group) was accompanied by satellite pulses, as shown in Figure 2.

After much experimentation, it was determined that 5 to 20 percent of the "true" electron pulses (in the main pulse) were accomplished by one or more after-pulses, delayed by about 1 to 100 μ sec. The presence of such a large number of afterpulses would be serious for any single electron counting application since it would cause an apparent increase in quantum efficiency without a true increase in utilization of input quanta. Furthermore, the mechanism of such afterpulsing would have to be understood if tube design were to be improved.

Several mechanisms, known to be possible, were postulated and checked:

- a. Visible fluorescence of the dynodes, especially in the anode region, leading to delayed feedback (delayed as a result of fluorescent decay time constants).
- b. Gas ion feedback
- c. Circuit (analyzer) misbehavior

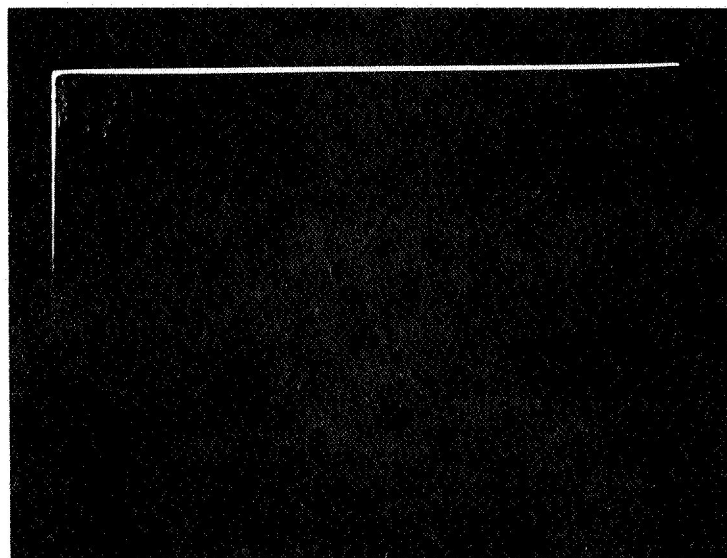


Figure 2

100 μ sec/cm; 0.05 volts/cm

0.1 sec exposure

- d. Soft x-ray fluorescent mechanisms
- e. Insulator charging effects.

After considerable experimentation it was finally determined that the light source itself (spark in dry nitrogen gas) was apparently showing residual luminescence, rather than MPT afterpulsing. While this possibility was not definitely confirmed observation of the output pulse from the FW-128 photodiode showed a pulse of about one-tenth the amplitude of and immediately following the main pulse. This effect was taken as a strong indication that there was, indeed, a problem with the light source.

2.0 AFTERPULSING INVESTIGATION

To further investigate the possibility of after pulsing in the multiplier phototube the equipment shown in Figure 3 was assembled. This arrangement eliminated the need for the triggered light source used previously.

A low intensity light source was used to excite single photoelectrons from the photocathode of an FW129 MPT, with a 14 mil IEPD², at a rate of about 1000 per second. These pulses are processed by the preamplifier and fed to the input of the multichannel analyzer (MCA) and the 547 oscilloscope. These pulses trigger the sweep of the oscilloscope and initiate the variable delay pulse which is applied to the coincidence input of the MCA. The MCA then analyzes only those pulses that follow the main single electron pulse by the preset delay time. In this experiment, the delay time was variable from 0 to 10 microseconds. The 541 oscilloscope is used to monitor the delay time.

Figure 4 is a plot of the single electron spectrum and dark count distribution for this tube, with the delaying pulse control set at zero. Figure 5 is a group of distributions obtained for delay times of 1, 2, 3 and 4 microseconds. Delays of longer duration do not contribute significant information. The low total number of counts for this data is an unfortunate consequence of insufficient counting time.

The distribution of these pulses is quite normal and show peak locations comparable with that of Figure 4 with the possible exception of that for 1 microsecond. In this distribution, there are about 10 times as many pulses in the early channels as there are in the region of the peak. While it is not possible to say with a high degree of certainty that these are indeed due to afterpulsing, there has been reported by Smith³ afterpulses with a delay time of 300 to 400 nanoseconds which may be attributed to H₂ ions. It remains to be shown that the observed pulses are in fact due to a similar cause.

While this experiment was being conducted, a sharp increase was noted in the number of pulses in channel one at a delay time of 4 microseconds and longer. It was further noted that the number of these coincident "afterpulses" was nearly the same as the total number of single electron pulses. After considerable investigation of this effect, it was discovered that there was positive overshoot of approximately 0.015 volts in the main pulse, as it appeared at the output of the preamplifier which occurred at 4 microseconds with the decay continuing well past 10 microseconds. It is not apparent at this point why such overshoot should count in channel one, especially since the analyzer input is not bipolar. The correspondence, however, between the number of these "afterpulses" and the main pulses is nonetheless disturbing. It appears that the resolution of this problem, and the one described in the previous section, may be a difficult equipment problem which is neither pertinent to nor within the scope of this contract.

2 Instantaneous effective photocathode diameter.

3 H. M. Smith, Jr., Photomultiplier Investigation Contract AT(30-1)-3421
RCA Laboratories, Princeton, N. J. 1966.

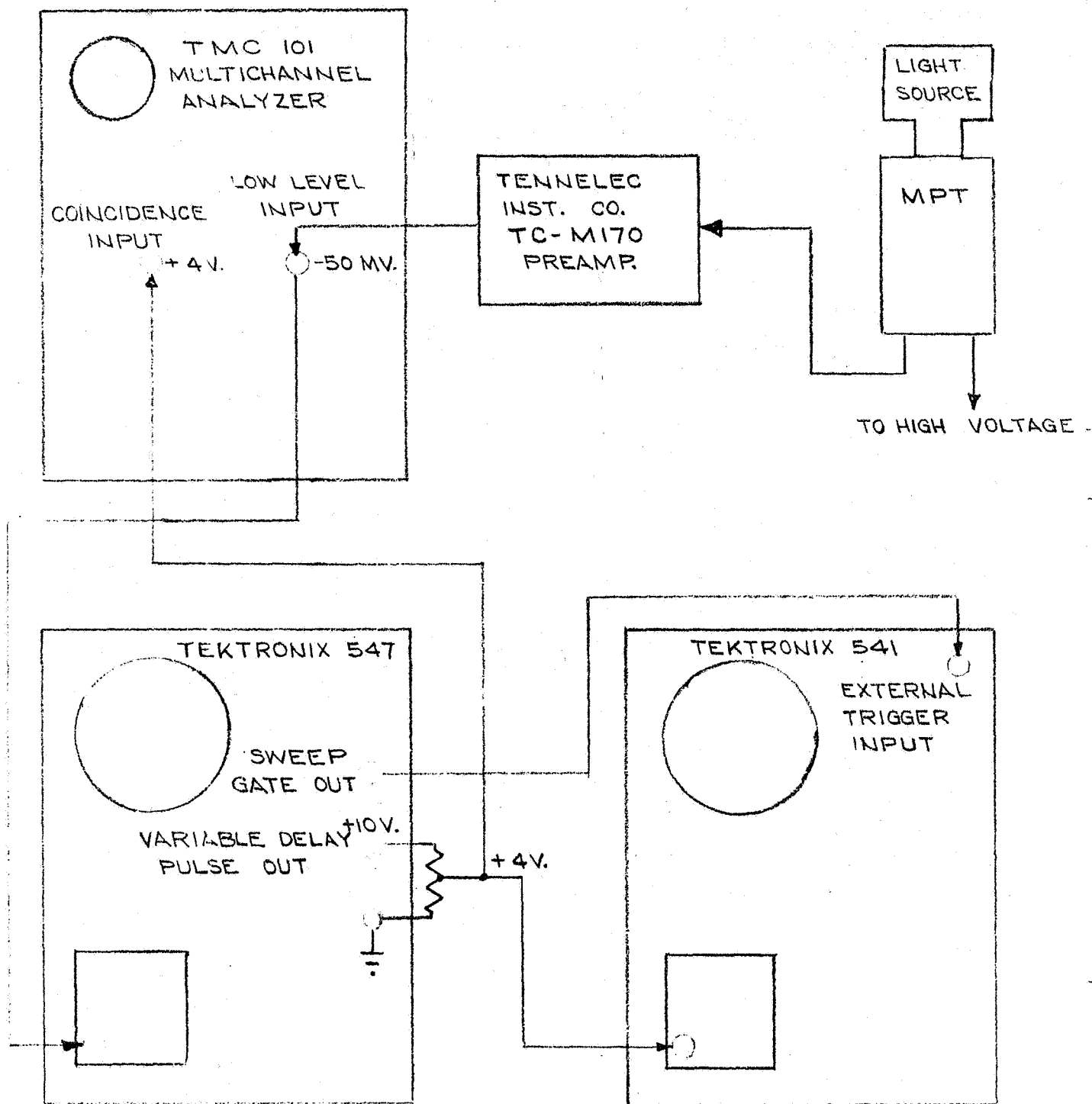


Figure 3

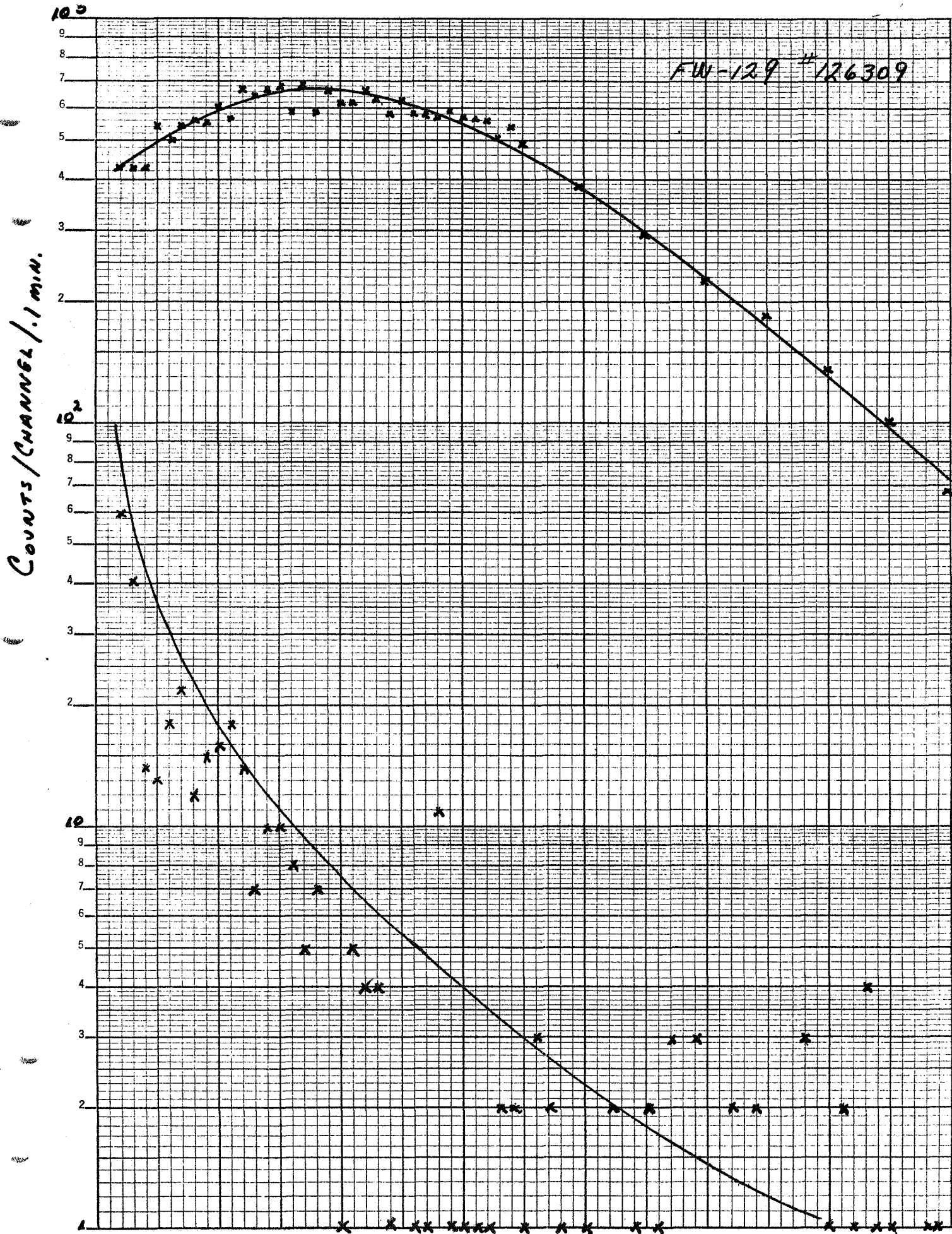


Figure 4

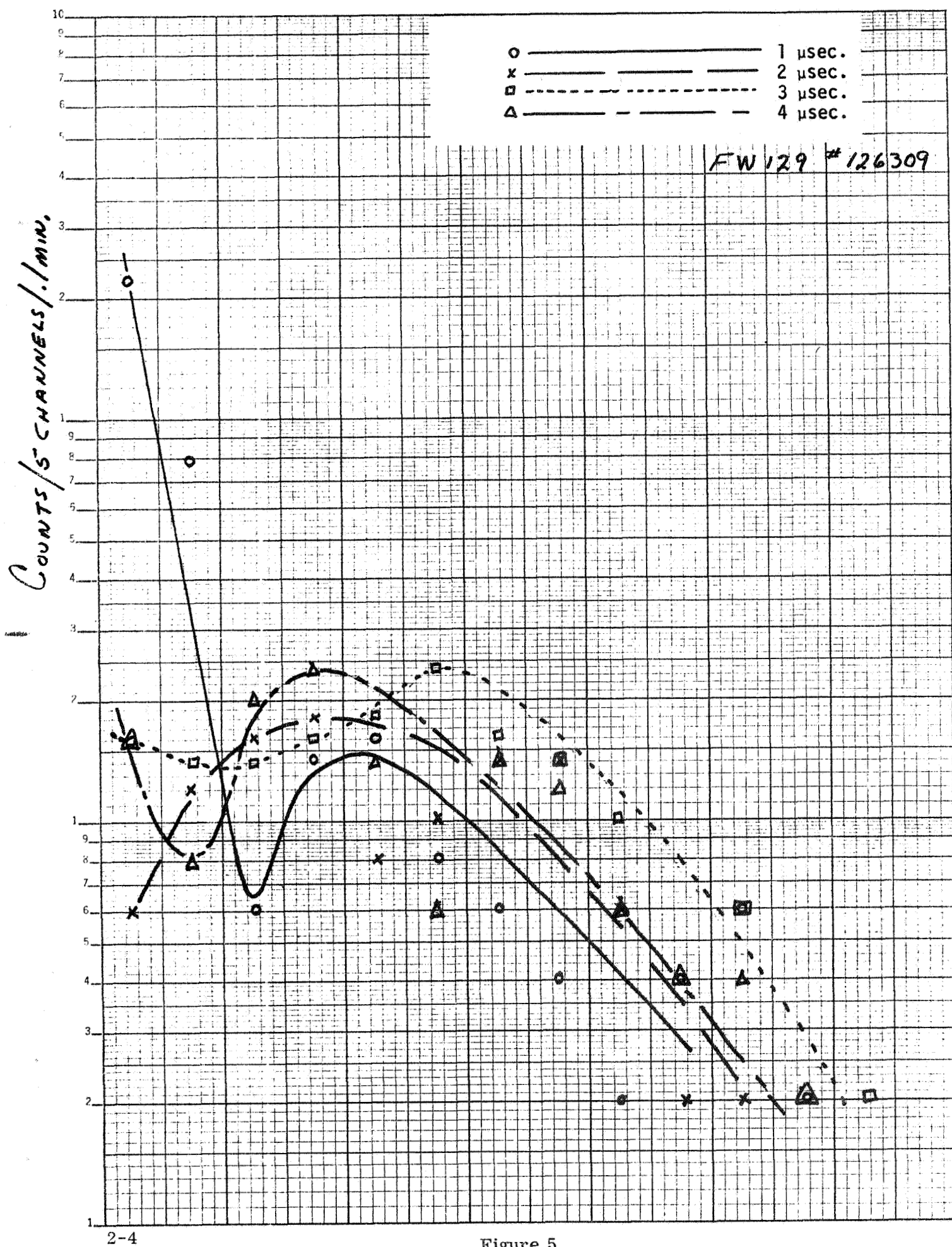


Figure 5

3.0 MATERIALS INVESTIGATION

3.1 Alkali Metals Used in Cathode Formation

It has been reported earlier⁴ that radioactive particles impinging on the photocathode entrance window gave rise to multielectron pulses due to fluorescence in the entrance window material. Since this problem appears to be worse in the case of a tube with an S-20 cathode an investigation of the materials used in forming this cathode was initiated.

A brief search in the literature gave a clue to a possible problem namely that K^{40} occurs naturally in potassium metal to the extent of 0.012 percent.

In view of this, two samples of the potassium chromate used in the cathode formation process, one of Fisher and the other of Mallenchrordt reagent grade were obtained. These samples were placed in a cast iron enclosure containing a Tracerlab Geiger tube type TGC-1 with a window thickness of 2.5 meg/cm² operated at 1450 volts. The output of the Geiger tube was fed to a Beckman model 2105 scaler.

In this test configuration the background counting rate was 40 to 50 counts in 5 minutes. With either sample of K_2CrO_4 the counting rate was 250 counts per 5 minute interval. With this information available, the most logical step was to identify the isotope. A scintillation counter was set up using a 3 inch Harshaw NaI crystal, a 8054 multiplier phototube and our multichannel analyzer. This equipment was operated for a 10 minute period with the K_2CrO_4 in front of the crystal. Figure 3 is the resulting spectrum showing the K^{40} photo peak at the far right. The peak near the center of the spectrum is a Cs^{137} peak added as a reference point. The gamma ray photon energy for K^{40} is 1.46 Mev while for Cs^{137} it is 0.662 Mev. While the scintillation counter is admittedly a rather crude arrangement, when compared to commercially available systems, the relative location of the two photo peaks in Figure 6, does seem to give clear evidence that K^{40} is a constituent of the material used in our S-20 photocathode processing.

A solution to this problem is, however, not easily attained nor is it known to what extent this possible source of multielectron pulses is at fault for the large pulse behavior of some ITTIL tubes. Isotopically pure K^{39} is available only in very small quantities as a byproduct of mass spectrometer separation processes and is therefore quite expensive approximately one dollar per milligram, a cost most phototube users would find prohibitive.

No such problem was found in the sodium chromate or cesium chromate also used in photocathode processing.

4 Final Report NASw-1058 Research in the Development of an Improved Multiplier Phototube Nov. 16, 1966.

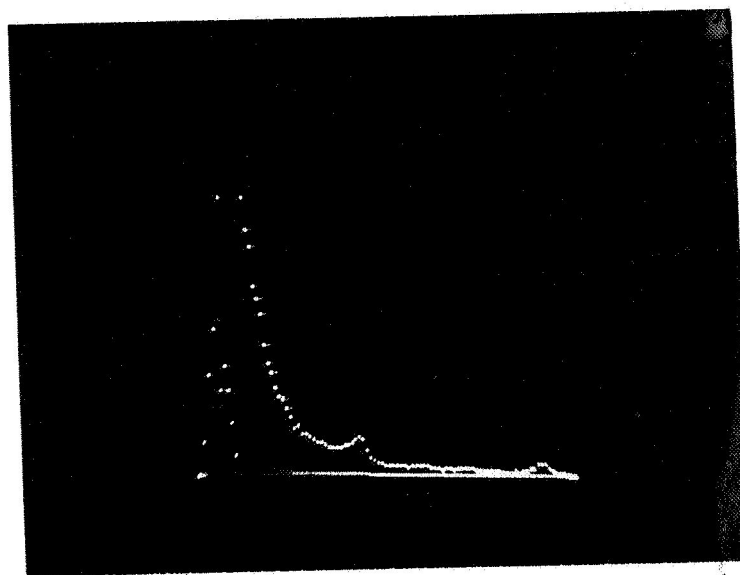


Figure 6

Composite K^{40} and Cs^{137} Gamma Radiation Spectrum

3.2 Faceplate Materials

Performance of multiplier phototubes in cosmic ray and other particle flux environments has already been reported^{5, 6}. However, the performance of materials and specifically, the relative scintillation rates of faceplate materials may be an important consideration in phototube design for specialized environments which cannot be determined from the reports. Moreover, the significance of scintillations may be great even for a nominally radiation-flux-free environment: potassium 40 is an S-20 photocathode constituent; it decays and produces a residual flux.

Scintillations were measured for the four (predominantly gamma) radiation sources and seven faceplate materials shown in Tables I and II. Cesium ¹³⁷, the only calibrated source, was used by itself and together with a 3/64 inch aluminum shield. Without the shield the cesium source emitted 2.7×10^6 gamma per minute.

An FW130 multiplier phototube which had a 0.350 inch diameter effective photocathode and 330 ± 35 dark pulses per second (at 80 to 90 percent counting efficiency) was used to count the scintillations; its photocathode was an S-20 type of 180 μ a/lumen luminous sensitivity deposited on a 0.080 inch thick 7056 glass faceplate.

For each radiation source a sequence of measurements was made in which the faceplate materials were successively interposed between the source and the phototube window. Intermittent determinations were made of the pulse rate which occurred when only the radiation source was positioned on the phototube window. All determinations were made over 0.1 minute live time intervals, at 80 to 90 percent counting efficiency and without illumination, but are reported simply as pulses per second. Representative pulse height spectra are included as Figures 7 and 8.

Generally, the gamma sources produced a marked increase in pulse rate for the FW130 multiplier phototube. The normal dark count (330 counts/second) may be compared to the "reference" (the radiation source present) levels shown in Table III. The pulse rate observed with a gamma source close to the tube decays to the normal dark count rate (within 5 percent) in about 5 minutes after the source is removed. The origin of radiation induced pulses is unclear: perhaps gamma or other particles interact with the multiplier or directly, with the photocathode as well as scintillating in the faceplate or walls.⁷ Another mechanism which has been proposed is soft x-ray production at the metal aperture cone followed by electron emission when the x-rays strike the dynodes.

5 A. T. Young, Rev. Sci. Instr. Vol. 37, No. 11, 1472 (1966).

6 C. Wolf, App. Opt. Vol. 5, No. 11, 1838 (1966).

7 A. J. Favale, F. J. Kuehne, and M. D. D'Agostino, IEEE Trans. Nucl. Sci., NS-14, No. 6, 190 (1967).

Table I Radiation Sources

<u>Source</u>	<u>Radiation Emitted</u>
Cs ¹³⁷	γ, β^-
Cs ¹³⁷ + 3/64" Al	$\gamma, (x\text{-rays?})$
Cd ¹⁰⁹	γ
Co ⁶⁰	γ, β^-

Table II Faceplate Materials

<u>Material</u>	<u>Thickness (In)</u>
fiber optic ¹	0.100
9741	0.080
7056	0.080
fiber optic ²	0.125
quartz ³	0.055
quartz ⁴	0.050
sapphire	0.050
1 uv transmitting	
2 non-uv transmitting	
3 fused	
4 crystalline	

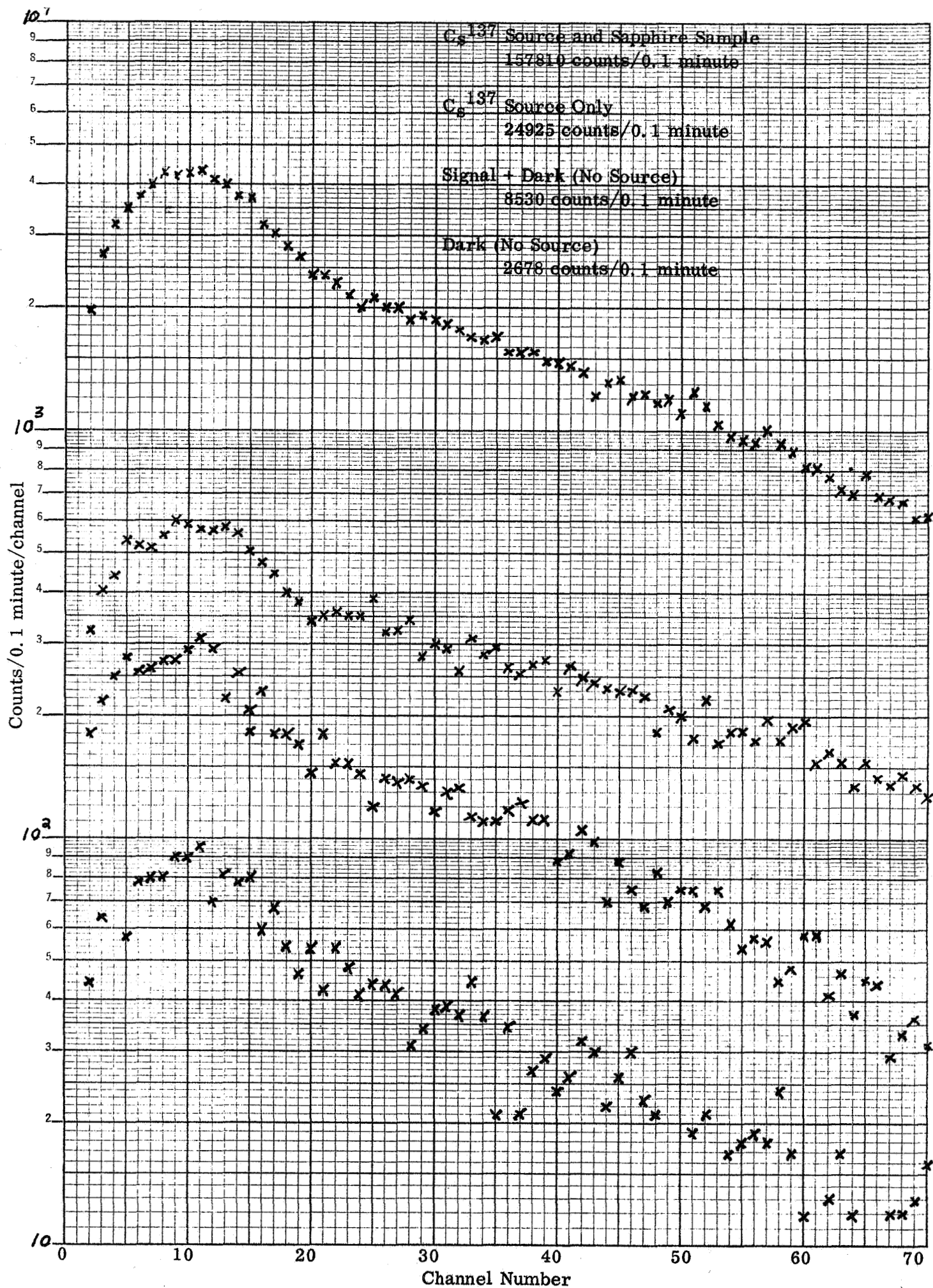


Figure 7

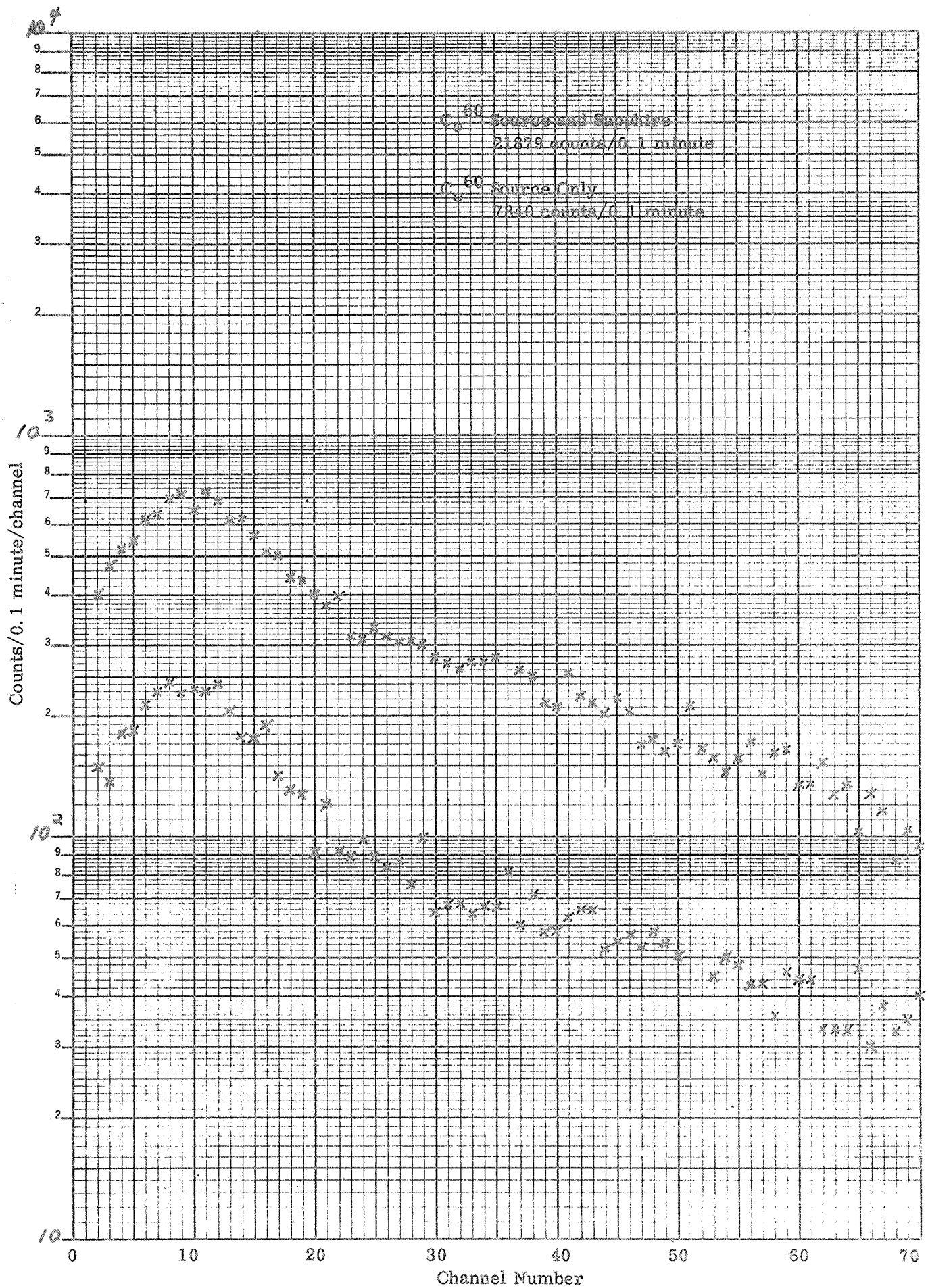


Table III Measured Pulses Per Second at 80 to 90 Percent
Multiplier Counting Efficiency

	C_s^{137}	$C_s^{137} + Al$	Cd^{109}	Co^{60}
reference	4154	472	34414	1245
fiber optic ¹	1684	344	23972	954
reference	4316	451	33651	1307
reference	4316	467	32292	920
9741	3941	445	28187	786
reference	4587	472	34414	2612
reference	4316	467	33802	976
fiber optic ²	2759	487	14205	722
reference	4587	472	33184	920
reference	4587	455	32812	727*
quartz ³	4538	427	23946	701*
reference	4521	467	28011	684*
reference	4587	439	32812	1060
7056	3540	401	19935	1372
reference	4521	455	28011	1221
reference	6251*	987(?)*	29659	754*
quartz ⁴	6237*	505*	20142	610*
reference	6714*	1017(?)*	33902	727*
reference	4587	464	28047	1221
sapphire	26302	2265	61650	3646
reference	4521	439	33221	858

* Analyzer and phototube gain were changed, so pulse rates are not readily comparable to others in table.

Sapphire scintillates strongly in gamma radiation fluxes. This conclusion is based upon the high pulse rates observed and the assumption that no anode pulse-producing gamma interactions other than scintillation take place in large numbers in sapphire. In fact, for cesium ¹³⁷, the number of scintillations counted was of the same order as the number of gamma rays emitted. This pulse rate, too, decayed as a function of time upon removal of the gamma source.

While the gamma sources themselves produced increased pulse rates, interposition of sample faceplate materials, other than sapphire, resulted in attenuation of the pulse rate as much as 50 percent. Some short-comings of the test method make actual attenuation by the material doubtful, however. The distance from the source to the phototube window increased whenever a sample material was interposed. This may account for the lowest pulse rates being registered for the thickest (fiber optic) faceplates.

4.0 COUNTING EFFICIENCY

An important consideration in the use of a multiplier phototube as a photon counter is the determination of its effective counting efficiency. For some time, it has been the practice in this laboratory to specify a tube capability in this regard for certain tubes in terms of the permissible number of dark count above a point equal to 20 percent of the single electron peak of the differential pulse height distribution curve. The statement of this information, however, does not indicate the efficiency with which the tube will count single events at the photocathode notwithstanding the fact that it is relatively easy to determine. On the other hand, the counting efficiency is a rather tedious calculation, though not difficult, to make on a routine basis for a pilot production run of tubes. For these reasons, it was decided to make an effort to correlate counting efficiency with some bias discriminator level location on the differential pulse height distribution in terms of a percentage of the single electron peak location. In order to accomplish this, a group of tubes with differing photocathode types and instantaneous effective photocathode diameters (IEPD's) were selected from standard tubes on which differential pulse height spectra had been run. The spectra were plotted on linear graph paper (Figure 9 through Figure 13) with each small division of the abscissa corresponding to one channel, but also divided into single electron pulse amplitude units. The distributions were extrapolated back to zero, as predicted by Poisson statistics, and a numerical integration performed. With this information, the counting efficiency curves were computed at intervals of five channels and plotted on the pulse height distributions. Inspection of these curves yields the information in Table IV. This indicates that, for the purpose of routine tests, a bias point of 60 percent of the single e^- spectrum peak yields a satisfactory counting efficiency figure of 85 percent. Our previous selection of 20 percent for the operating bias point may therefore be considered as too conservative, i. e. leading to too high dark counting rate.

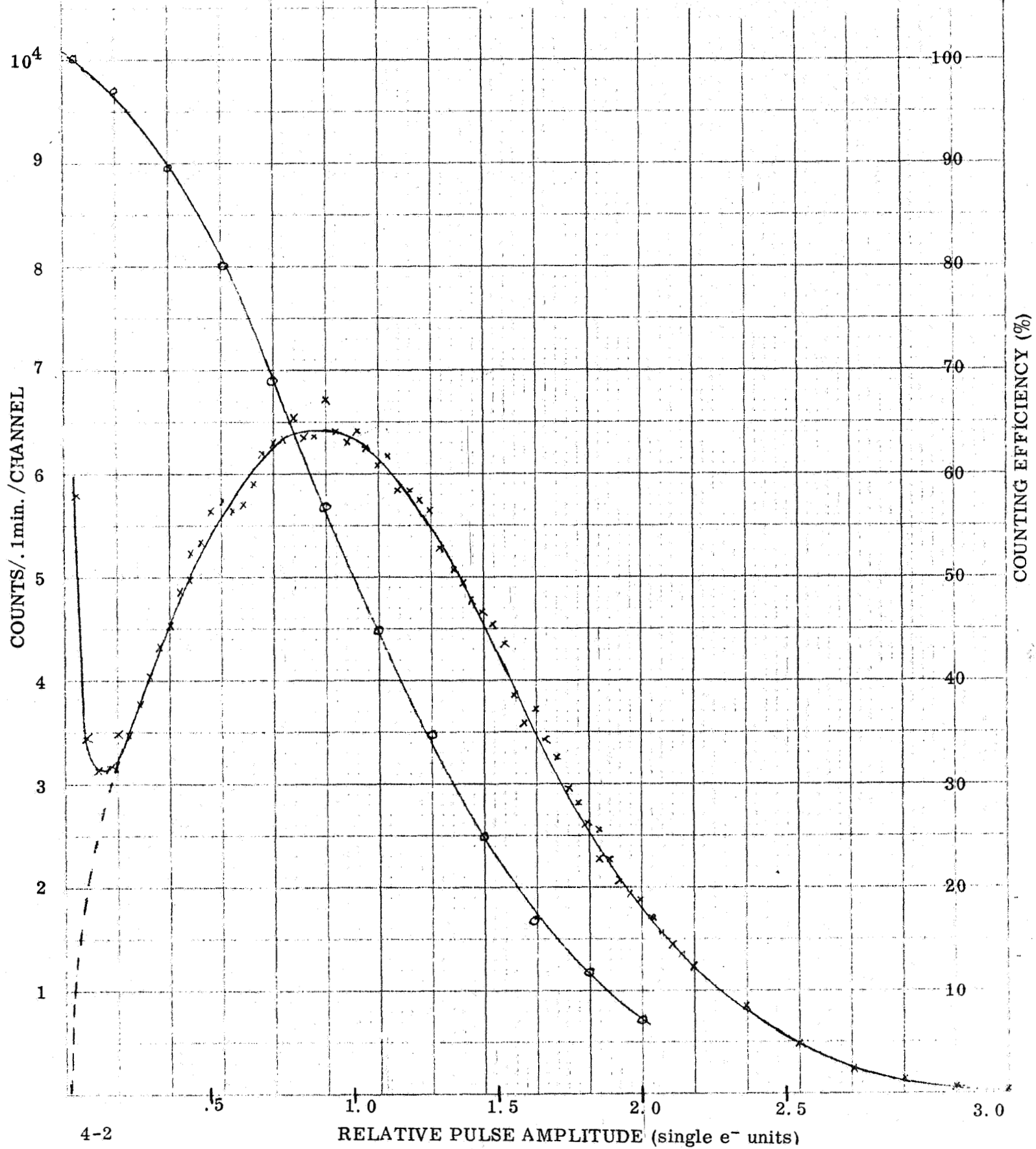
4.1 Light Source Calibration

The concept of using a radiation detector to count individual input quanta (upon which the present contractual effort is based) introduces, almost automatically, the concept of "counting efficiency". This counting efficiency is just the ratio of recorded output counts to the number of input quanta for a given observation time. It differs from the ordinary concept of "quantum-efficiency" as applied to photodiodes and photocathodes in that quantum-efficiency as usually defined is computed from average rate of photocurrent flow measurements (for example using ammeters) rather than using true counting registers.

FW129 No. 126309 IEPD = 0.014

1 Channel = 0.037 Single e^- units

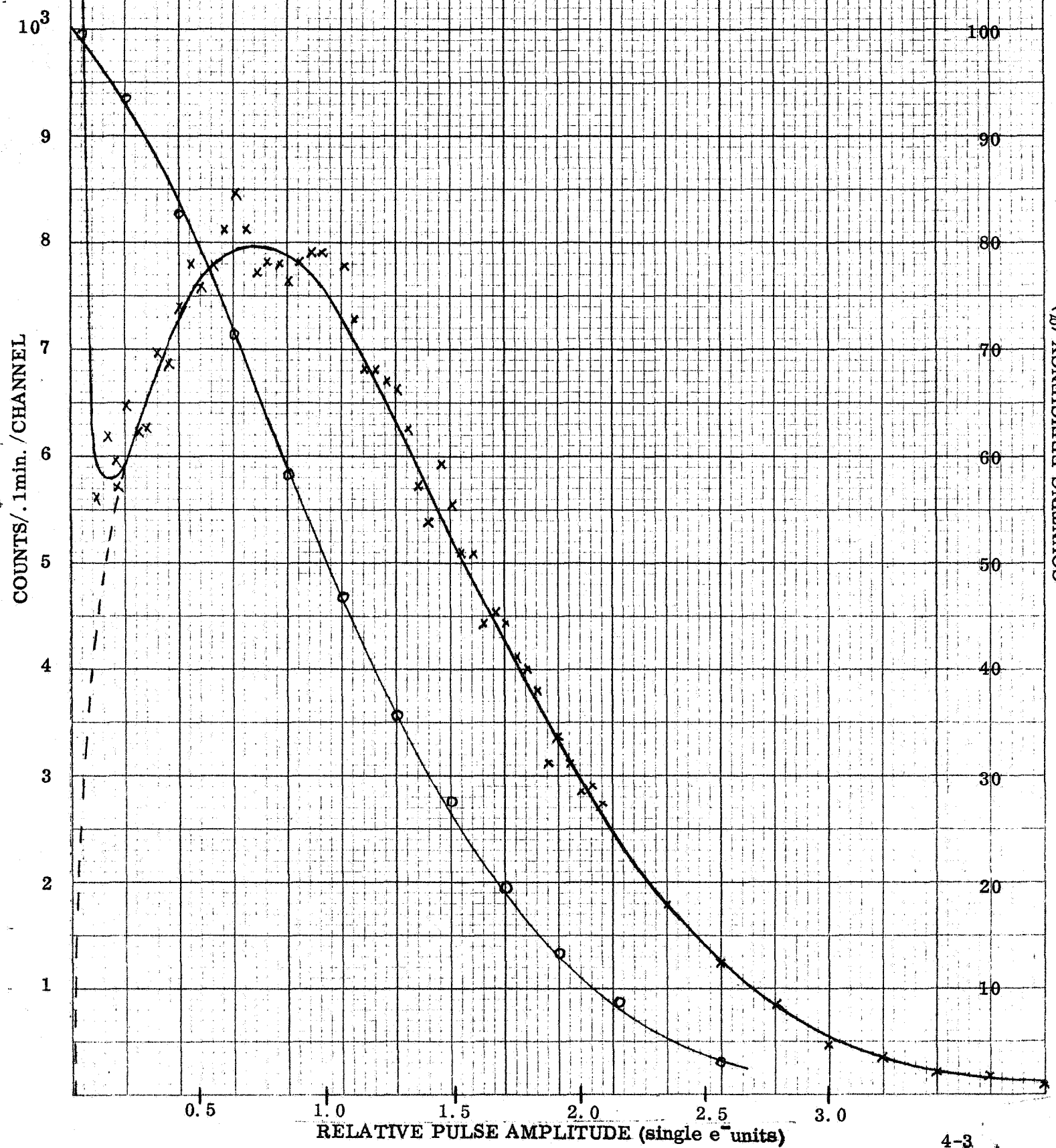
Figure 9



FW118 No. 116616 IEPD = 0.350

1 Channel = 0.043 Single e^- units

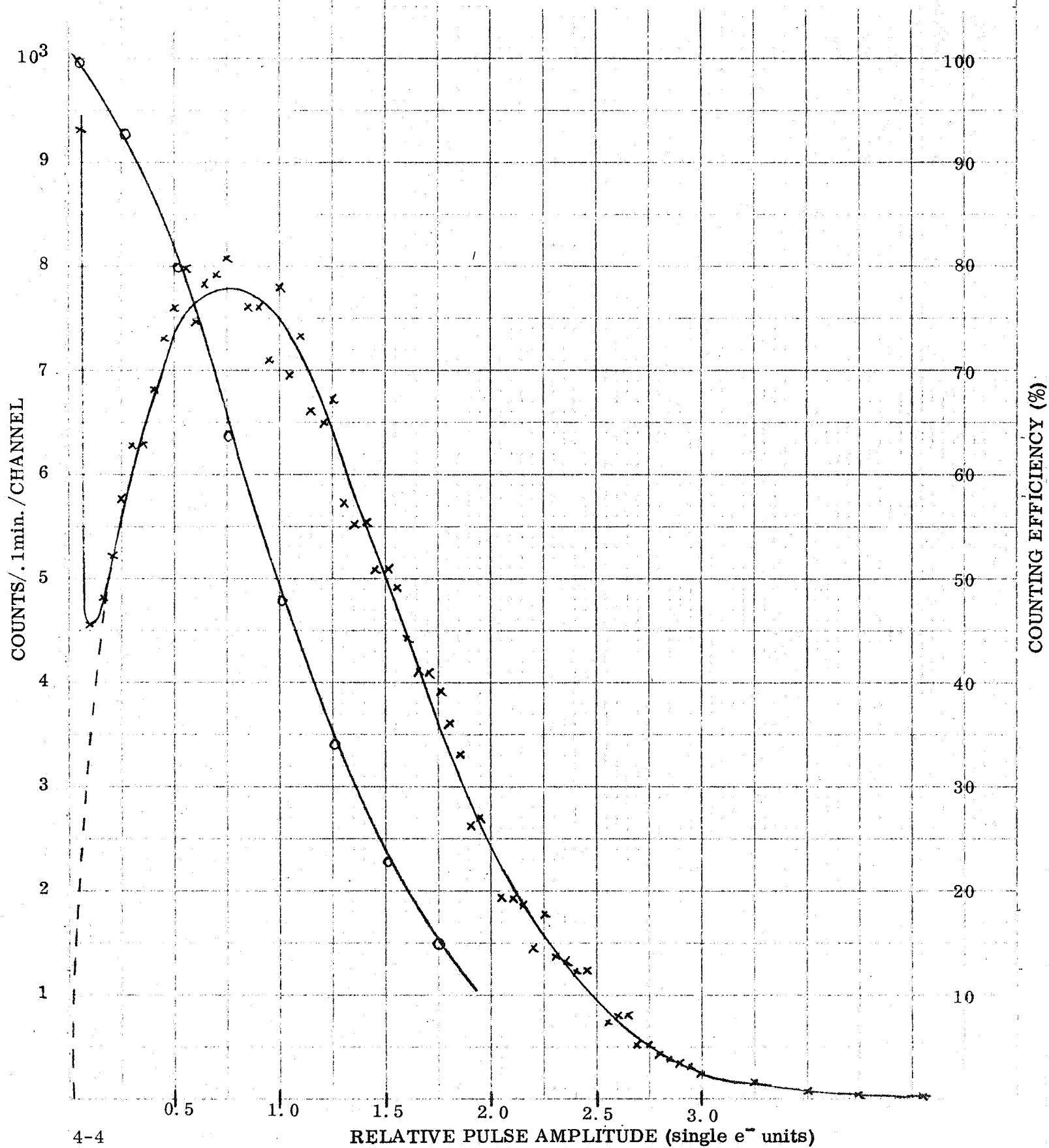
Figure 10



FW130 No. 126603 IEPD = 0.100

1 Channel = .05 Single e^- units

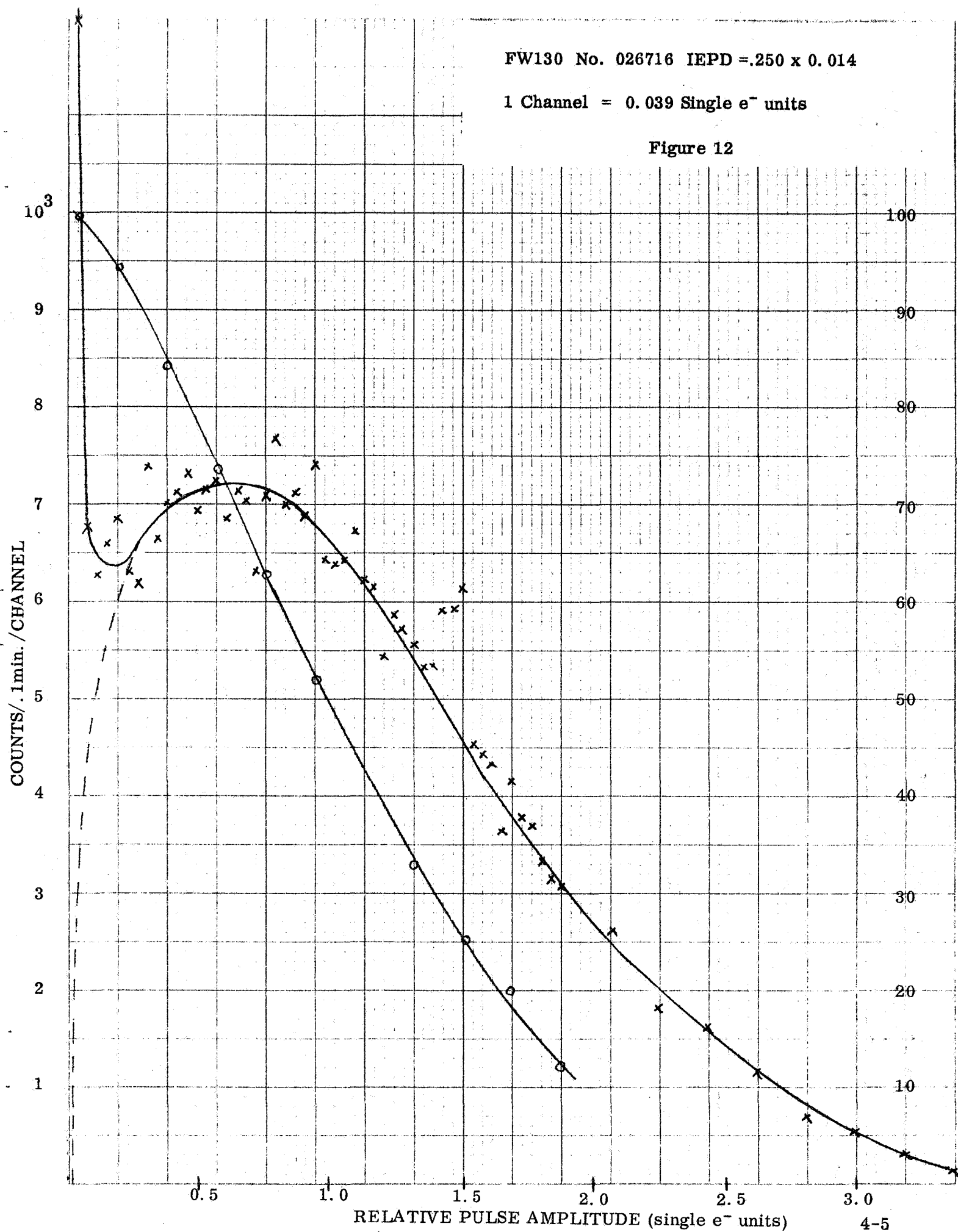
Figure 11



FW130 No. 026716 IEPD = .250 x 0.014

1 Channel = 0.039 Single e^- units

Figure 12



1 Channel = 0.031 Single e^- units

Figure 13

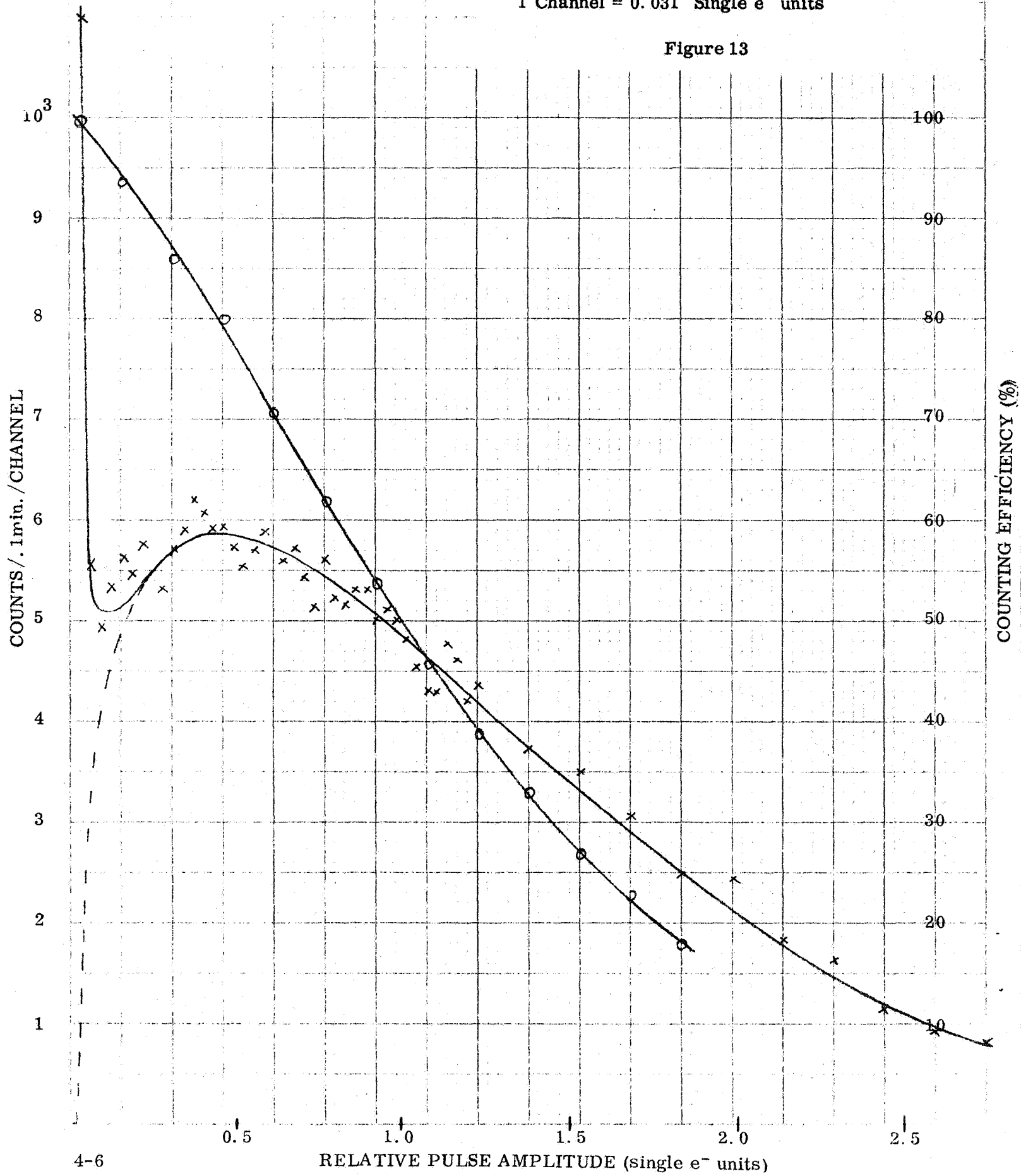


Table IV

Tube No.	IEPD	Counting Efficiency	Percent of Single e ⁻ Peak	Measured Total Dark Count @ 85% C. E.
FW129 No. 126309	0.014	85%	63%	0 @ 24°C
FW118 No. 116616	0.350	85%	59%	3 @ 70°C
FW130 No. 126603	0.100	85%	60%	7 @ 24°C
FW130 No. 026716	0.250 x 0.019	85%	62%	6 @ 24°C
FW130 No. 026723	0.350	85%	65%	890 @ 24°C

Average % of Single e⁻ Peak 62%

Thus, in evaluating a radiation detector as a quantum counter it would be highly advantageous to devise a means by which the counting efficiency could be measured directly. In general this involves the far-from-trivial problem of generating a flux source of known properties at a sufficiently low-flux level (usually less than 10^6 photons/second) so that accurate counting of the output pulses from the detector can be made without accidental overlapping of pulses.

The general test configuration we have selected for this purpose is shown in Figure 14.

In use, the number of counts, N , recorded by the counting register for an observation time, T , is recorded, and the counting efficiency, E , for the wavelength, λ , computed from:

$$E = \frac{N}{T F_{\lambda}}$$

where F_{λ} is the known rate of quanta production from the test flux source.

4.1.1 Calibration Principles

Without discussing in detail the many possible methods of determining the magnitude of the test flux level, F_{λ} , the particular procedure we have followed can be outlined as follows:

- a. Measure the quantum efficiency of the photocathode of a suitable MPT tube at sufficiently high test flux levels so that conventional equipment can be used. (Linearity of cathode response is assumed).
- b. Measure the differential single electron pulse height distribution of an MPT showing the highest possible peak-to-valley ratio, a low dark counting rate, and a Poisson-derived pulse amplitude distribution.
- c. Predict the absolute counting efficiency of the multiplier section of this tube (all sections following the photocathode) based on an extrapolation of the single electron differential pulse height distribution to zero amplitude (see Figure 15a) or on an extrapolation of the plateau of the corresponding integral pulse height distribution to zero amplitude as in Figure 15b.

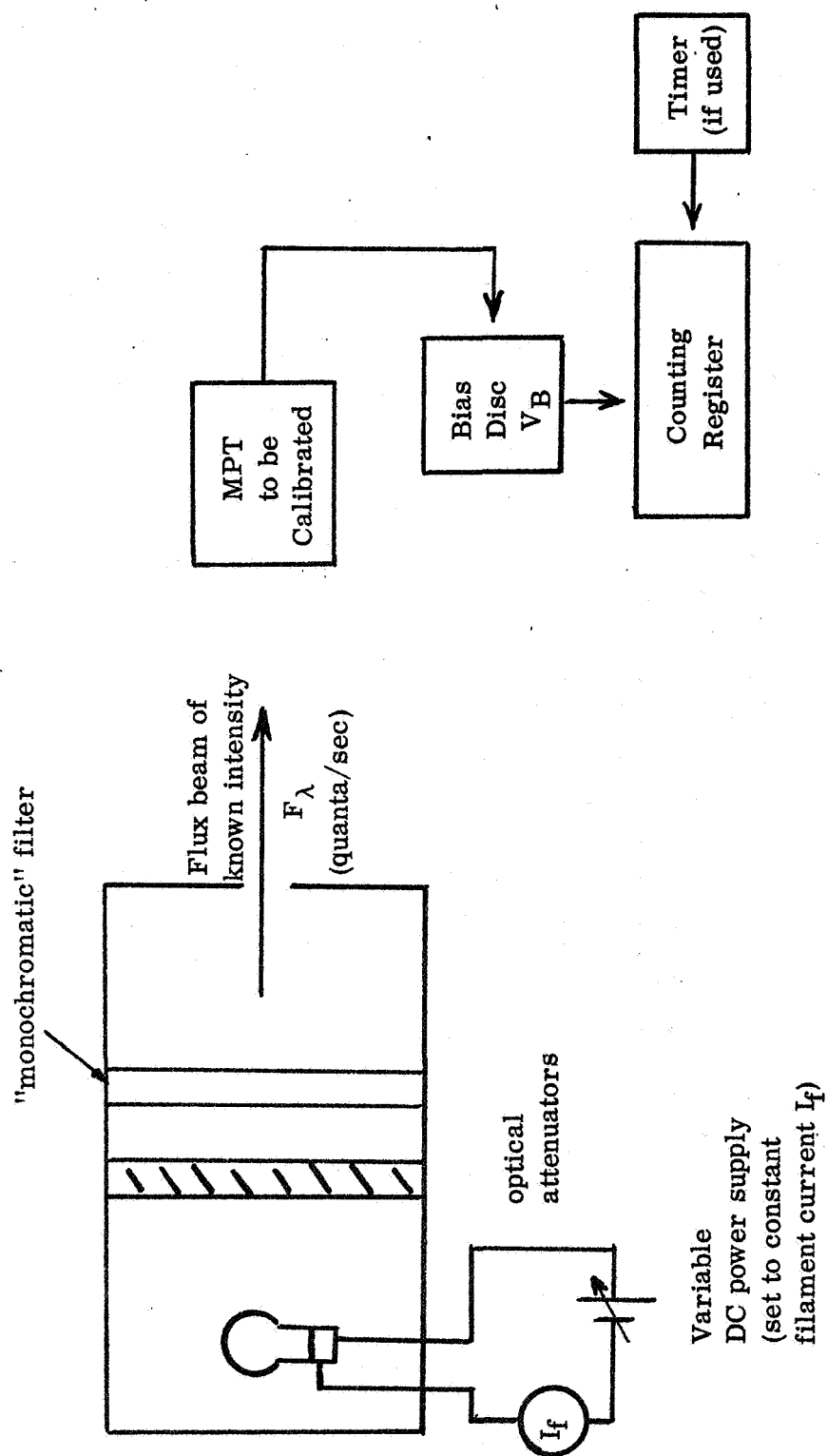


Figure 14 Counting Efficiency Test Configuration

$$Q_m = [1 - p(o)] \frac{A_2}{A_1 + A_2}$$

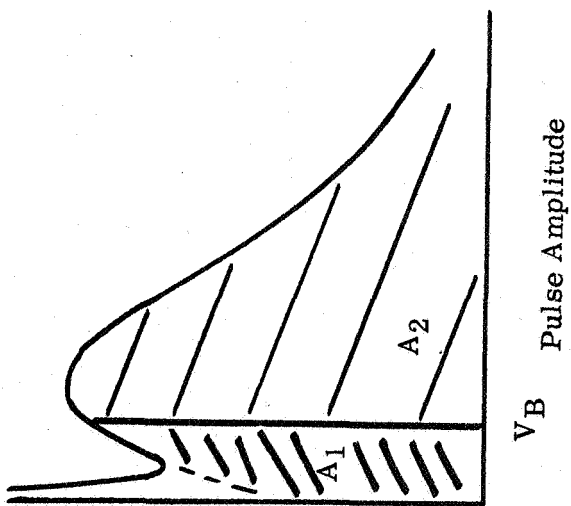


Figure 15a Differential Distribution

$$Q_m = [1 - p(o)] \frac{N_B}{N_O}$$

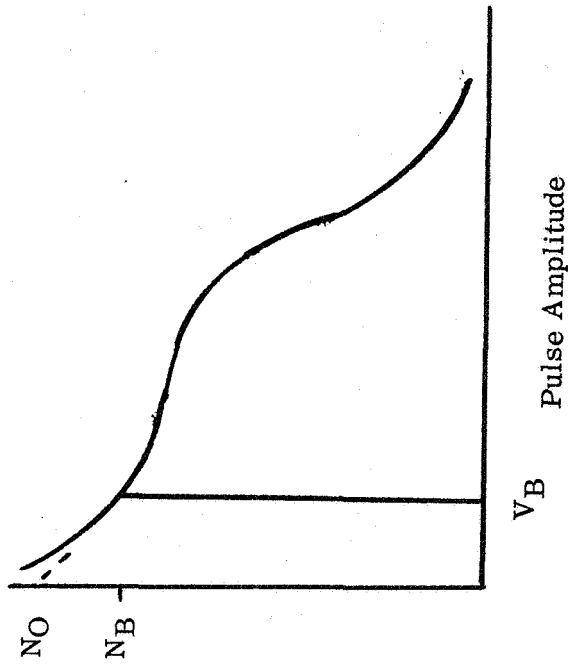


Figure 15b Integral Distribution

The relative number of counts $A_2/(A_1 + A_2)$ recorded under the resulting bias discriminator bounded extrapolated curves in Figure 15a or the ordinate counts N_B/N_0 in Figure 15b is then assumed to be approximately the "true counting efficiency" Q_m of the multiplier. If so desired it is possible to estimate a value for the magnitude of $p(0)$, the finite probability that a photoelectron striking the first dynode (D1) will eject no secondary electrons, but this value should be kept small (less than 0.05) by operating at a high voltage between photocathode and D1 and by maintaining a good, high yield surface on D1.

Areas where the critical probabilistic processes of photoemission, secondary emission and bias discrimination take place are indicated in Figure 16.

The overall counting efficiency E of the tube used for calibration at some practical bias discrimination level, V_B , is then assumed to be given by:

$$E = QQ_m = Q [1 - p(0)] \frac{A_2}{A_1 + A_2}$$

where Q designates the photocathode quantum efficiency.

This assumed absolute counting efficiency can then be used to determine the test flux, F_λ .

It is clear that this method of calibration is, in reality, nothing more than a comparison between the counting efficiency of a tube being tested and the counting efficiency of a selected tube used for calibration. Until more accurate procedures for determining F_λ become available, this comparison method will probably have to suffice. It does have the merit of allowing us to rank "good" tubes according to their merit for quantum counting, and to recognize test situations in which anomalously high counting efficiencies (sometimes apparently greater than 100 percent) are encountered (true for many MPT tubes as $V_B \rightarrow 0$).

4.1.2 Specific Calibration Procedure

The low light level source which has been used at ITTIL in quantum counting was modified by inserting an interference bandpass filter at 600 nm between the bulb and the first (pinhole) aperture. The filter has a half-power wavelength of 15 nm. An approximate calibration of a test flux level was obtained, as indicated above, by using an FW130 multiplier phototube as a transfer standard, from a Leiss and a filter monochromator.

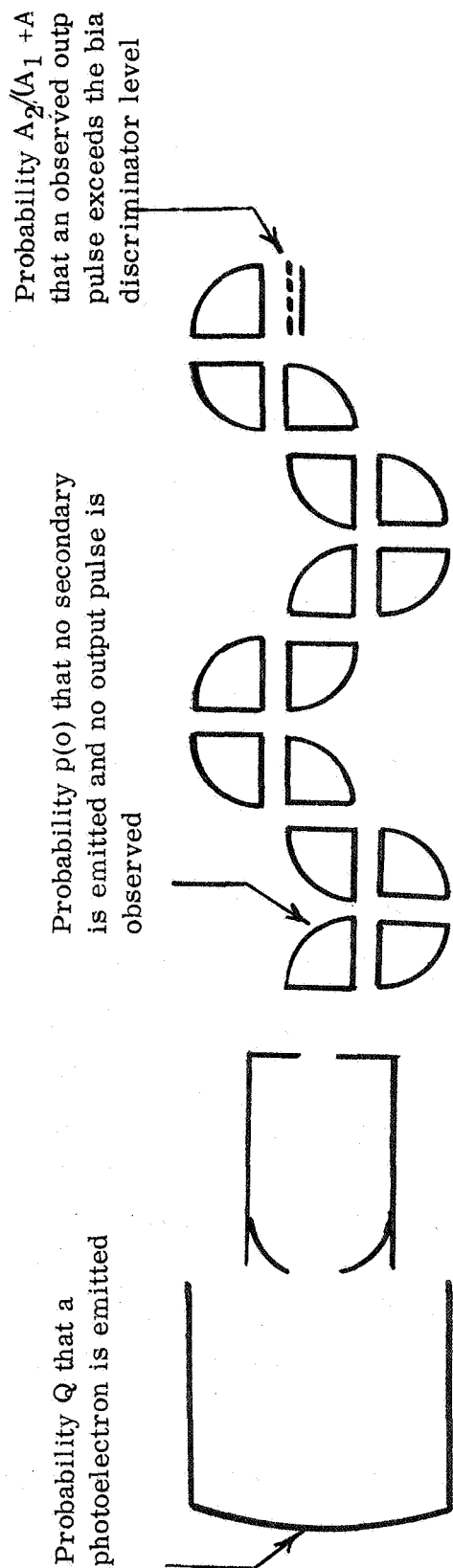


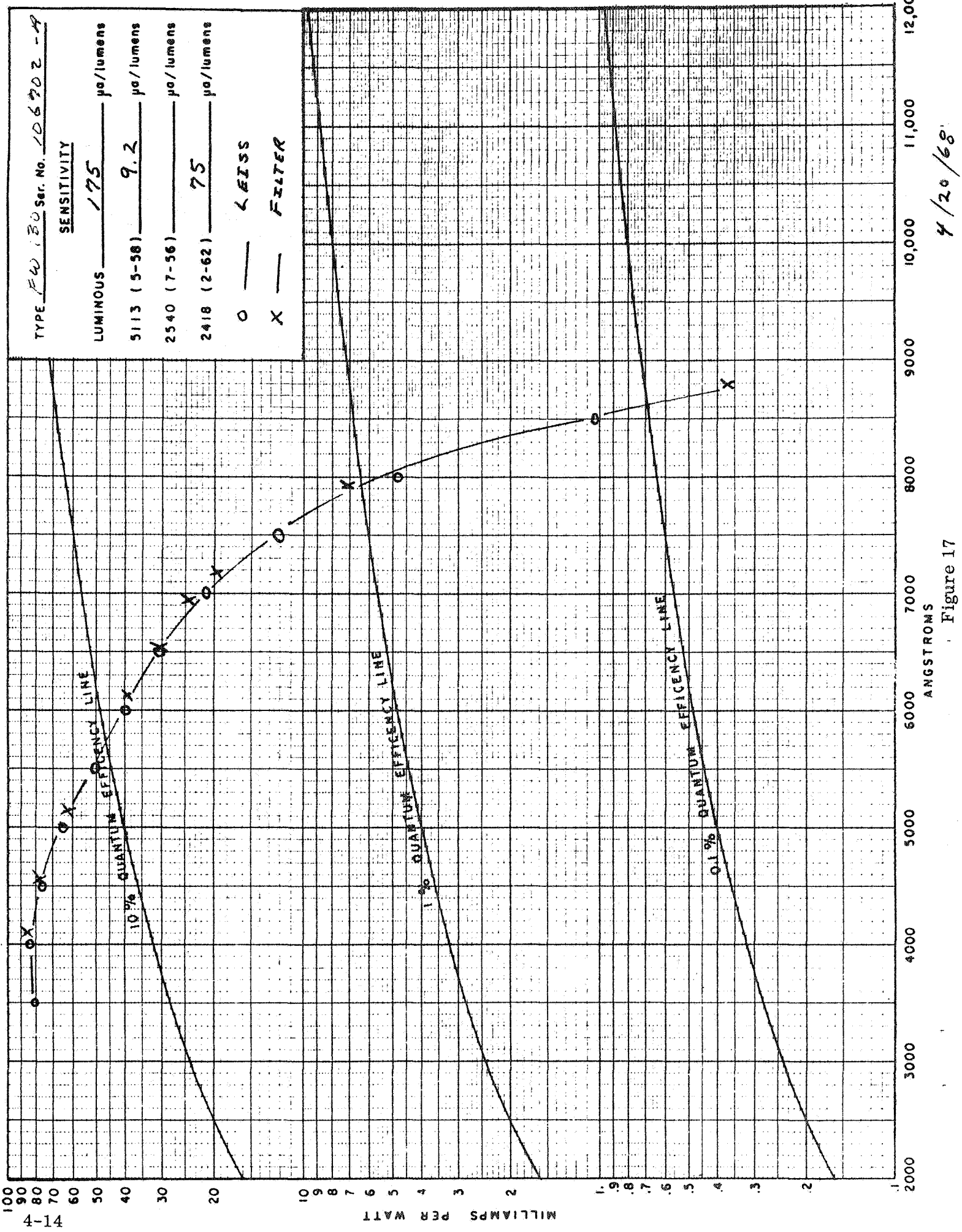
Figure 16 Configuration of the FW130 Phototube and Event Probabilities For a Single Incident Quanta

The FW130 used was No. 106702 which has a 0.350 inch diameter effective photocathode and a cathode luminous sensitivity of $175 \mu\text{a/lumen}$. The photocathode spectral response (Figure 17), determined from the Leiss and filter indicates a photocathode quantum efficiency of $8.2 \text{ percent} \pm 0.4 \text{ percent}$ at the peak wavelength of the filter (600 nm).

Signal plus dark and dark pulse height distributions were obtained with 1 minute live counting time and were used to compute signal differential and integral distributions (Figure 18). The signal differential peak occurred in channel 25 indicating that a pulse height bias discriminator level nominally chosen equal to 60 percent of peak would be channel 15. A dark pulse rate of 225 ± 30 counts per second was observed at this bias level. The number of signal counts per second and the approximate multiplier "true counting efficiency" (also at 60 percent bias) were determined to be 211 counts/second and 86.0 percent for the chosen flux level. (A second and higher flux level was also calibrated: signal 3606 counts/second and 80.2 percent for the higher level. The pulse height spectrum is shown in Figure 19.) The probability $p(0)$ that a photoelectron which strikes the first dynode will eject no secondary electrons for a silver-magnesium surface and a 230 electron-volt incident energy has been determined by Bay and Papp⁸ to be about 2.8 percent. A 200 volt image section voltage was used and so the above is a reasonable approximation. The true multiplier counting efficiency corrected from above by multiplying by $(1 - p(0))$, is 83.6 percent (77.9 percent for the higher flux level).

The overall counting efficiencies may be easily calculated to be 6.8 percent and 6.4 percent and hence the light fluxes are 3106 and 5634 photons per second for the 0.0963 cm^2 effective cathode area or 3226 and 5850 photons per second per cm^2 .

The procedure indicated above allows phototubes to be ranked relative to tube No. 106702 in their quantum counting abilities. But more than that it places proper emphasis upon the critical role of the dynodes in producing a peaked signal differential pulse height spectrum, a spectrum which may be validly extrapolated as in Figure 15a or 15b, and in affecting the overall counting (or quantum) efficiency of a multiplier phototube.



4/20/68

Figure 17

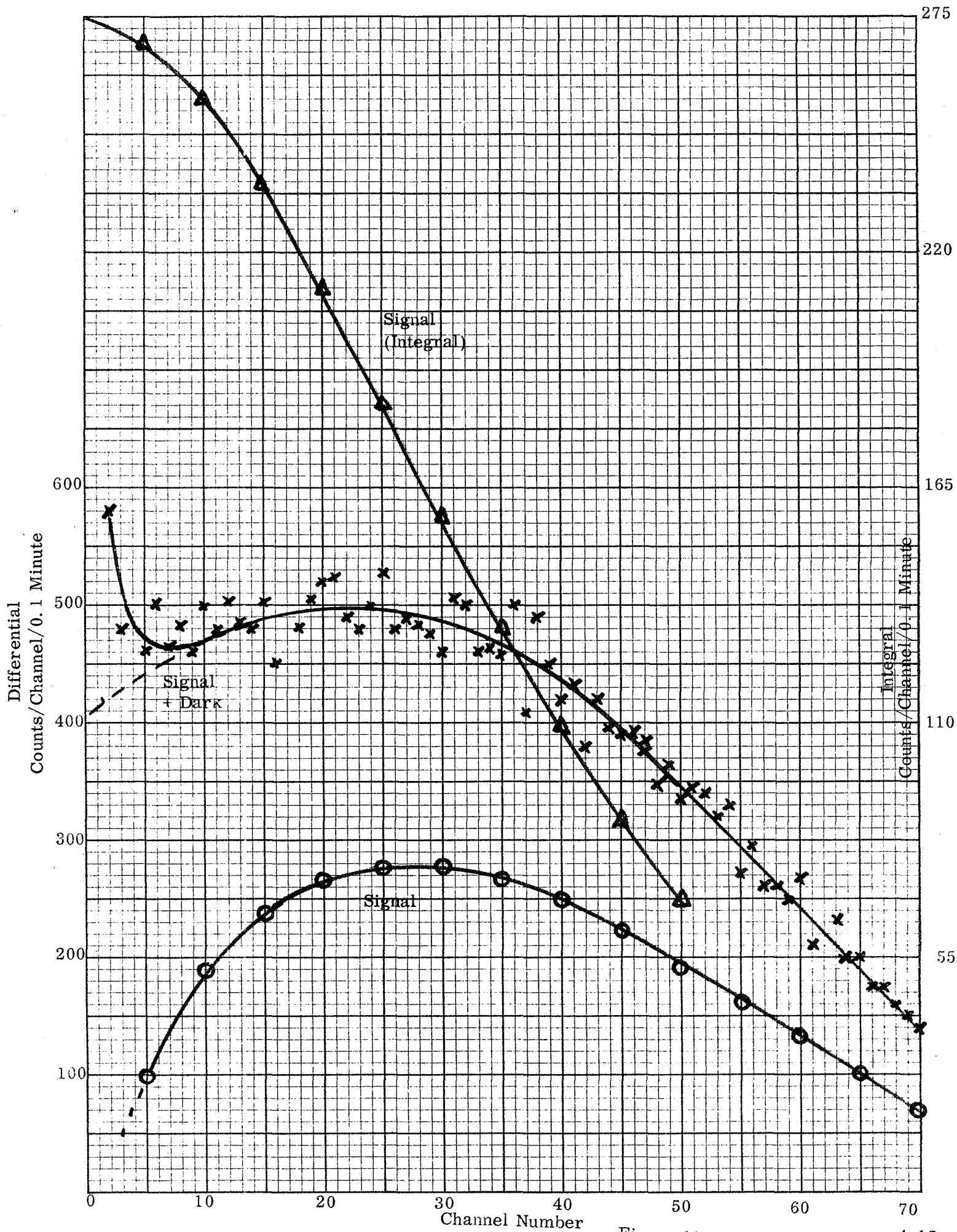
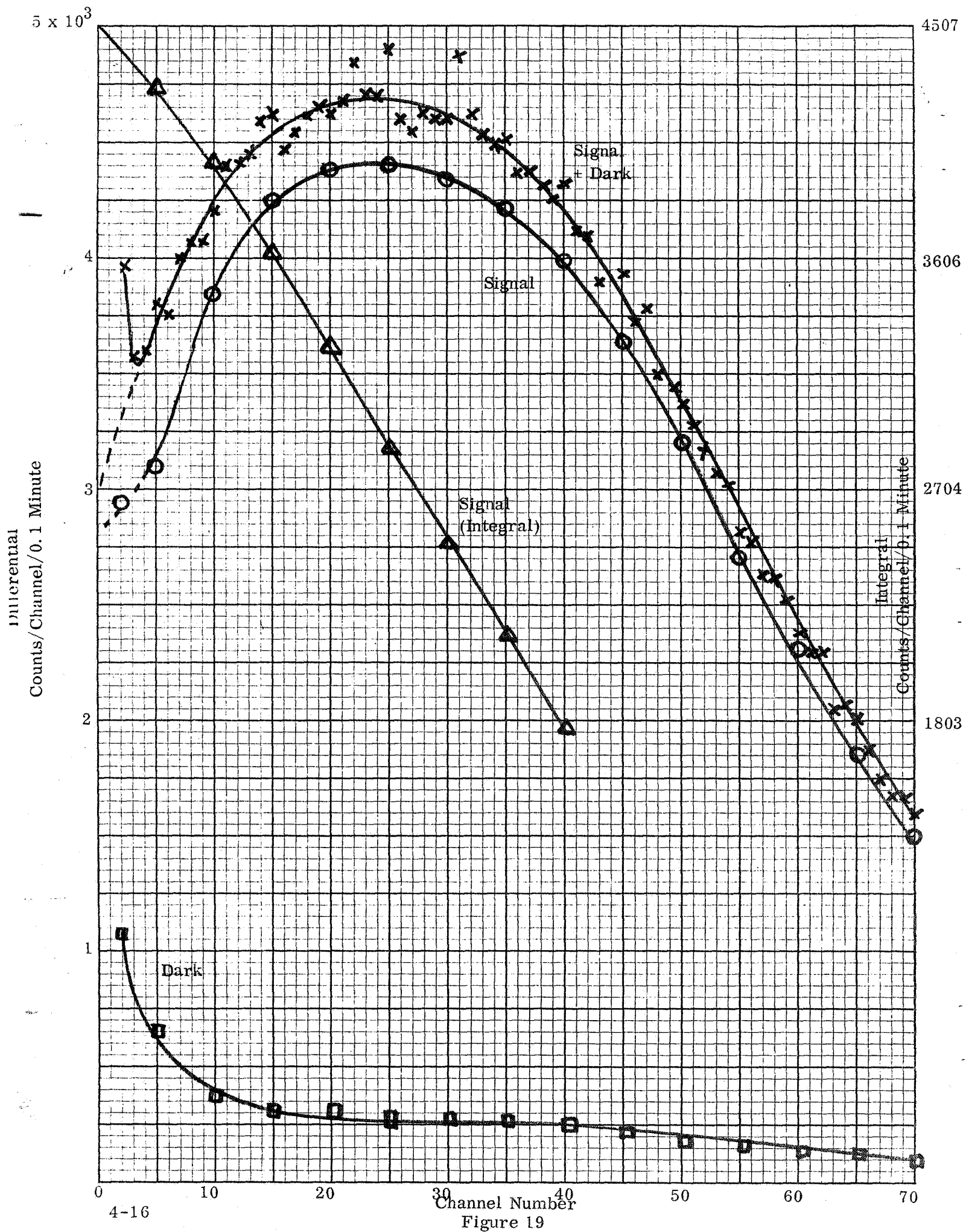


Figure 18



5.0 SPECIAL MULTIPLIER TYPES

There are certain other multipliers, with special characteristics, which have been developed by ITTIL but which may also be useful in photon counting applications.

Of these special types, two tube types were tested, the F4034 fast rise multiplier phototube and the F4036 electron multiplier.

5.1 Fast Rise Time Multipliers

The F4034 is a ten-stage multiplier phototube with a focused multiplier rather than the box and grid type used in the FW130. It has an image section ahead of dynode one which has been modified so that electrostatic focusing of the electron beam is possible. The anode terminal is a 50 ohm coaxial connector brought out at the center of the tube base. A photograph of the F4034 is shown in Figure 20. These tubes are capable of delivering high current linear output pulses, with a rise time of the order of 1 nanosecond, into 50-ohm loads. They are also capable of detecting light sources pulsed at very high frequencies. Typical output characteristics for the F4034 are shown in Figure 21. Because of these characteristics, it seemed advisable to investigate their statistics for possible use as high speed single photon counters. As such, they would have a markedly increased dynamic range for the input photon rate level.

Figure 22 shows the voltage divider used for rise time and anode response. The configuration of the divider was the same for all tests. In particular, the determination of rise time requires that the anode be operated at a more positive potential than the accelerator grid and that the dynodes be bypassed in order to avoid space charge limiting of the output current and to achieve optimum frequency response. Other standard tests such as ENI, and dark current do not require the dynode bypass capacitors and external anode bias. A pulse height distribution for single electrons from the photocathode of F4034 No. 086702 is shown in Figure 23. The total dark count for this tube was 184 counts in 6 seconds. If the method described previously (page 4-1) for determining the dark counting rate at counting efficiency of 85 percent is applied, it will be seen that there are just seven dark counts per second.

A contradiction exists between the data for this tube and a similar tube (No. 056706), still undergoing evaluation, in that comparable dark counting rates are obtained for both tubes with quite different focus potentials. The focus electrode of Tube No. 056706 was operated at -21 volts with respect to cathode while for Tube No. 086702 it was operated at cathode potential even though the optimum focus potential is about -20 volts with respect to cathode, for 2500 volts overall, as indicated by maximum anode responsivity. Figure 24 is a curve showing the variation in total dark counts for Tube No. 086702. This data indicates that when a voltage is applied across

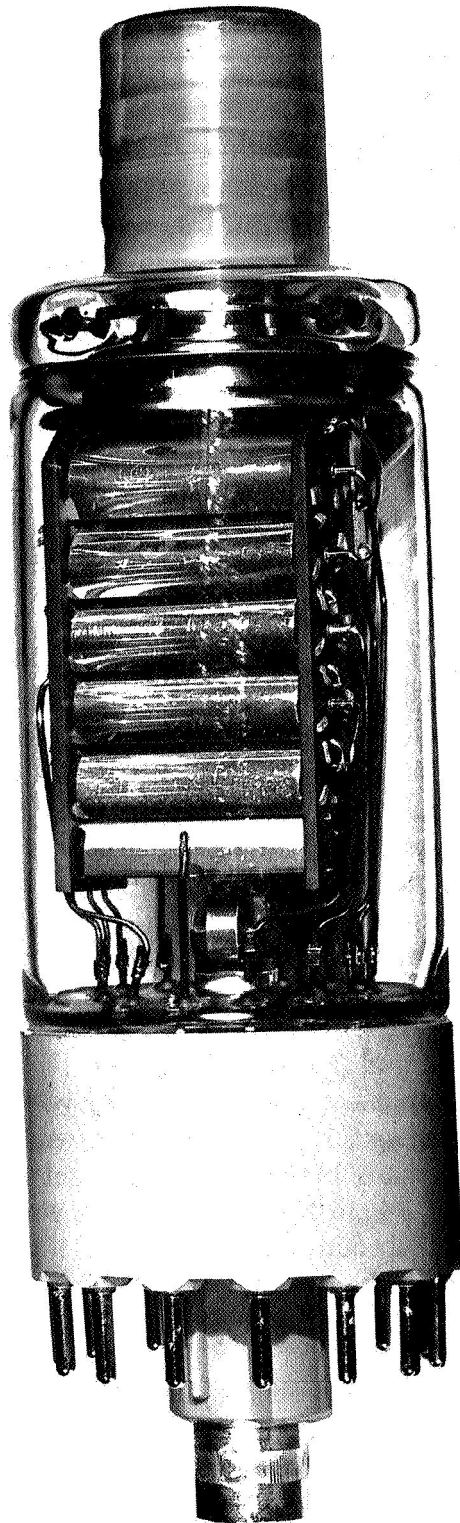


Figure 20 F4034

Pulse Response F4034 Serial No. 086702

Voltage Divider ----- See Figure 5

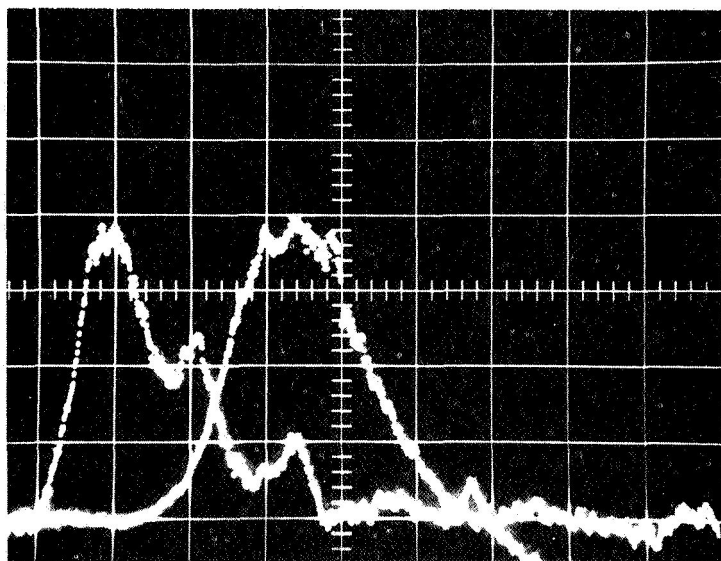
Divider Voltage ----- 3400

Anode Bias ----- 270V

Horizontal Calibration ----- 1 nanosec./cm

Vertical Calibration ----- 1 volt/cm
(Photomultiplier output only)

Anode Load ----- 50 Ohms



First Trace ----- Spark Gap viewed with F4014 ultra fast photodiode

Second Trace ----- Spark Gap viewed with F4034 S/N 086702

Figure 21

VOLTAGE DIVIDER USED
TO TEST MULTIPLIER PHOTOTUBE
TYPE F4034

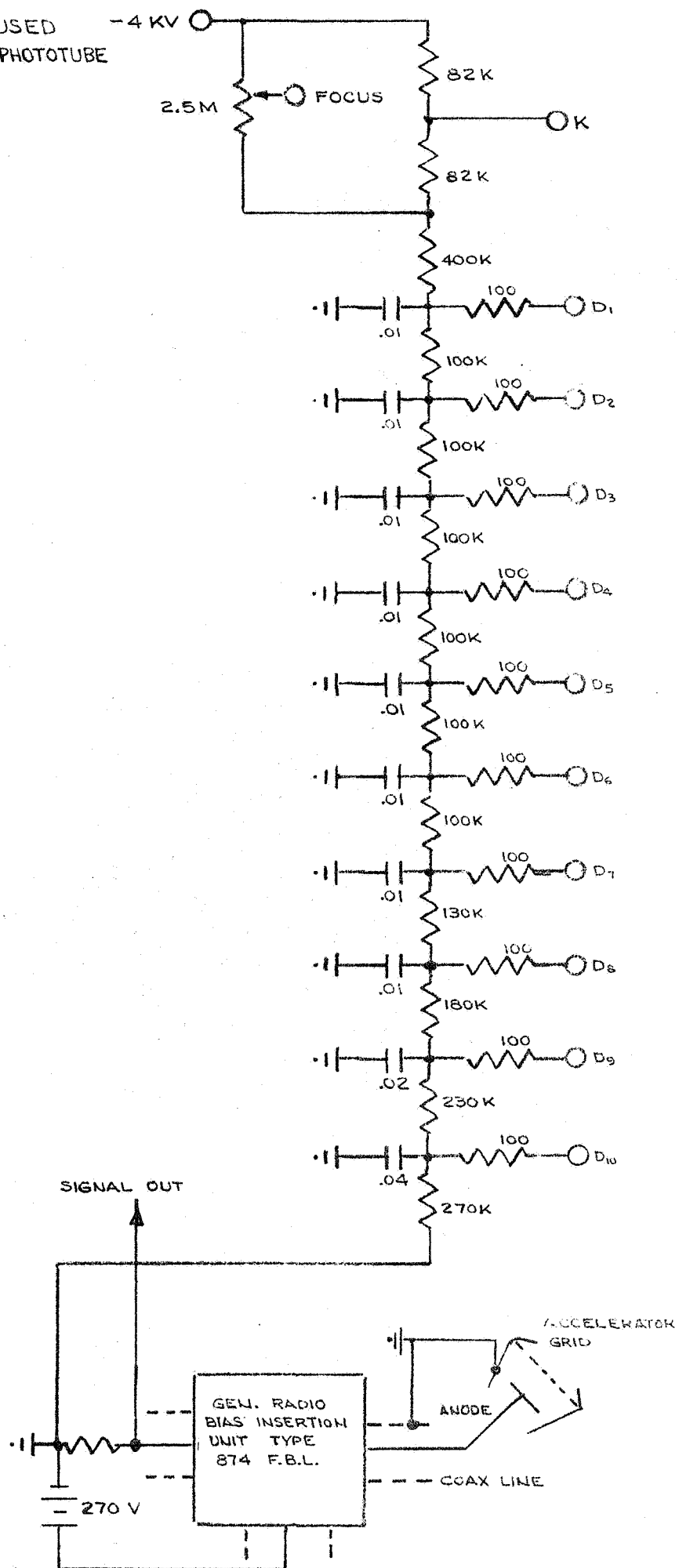


Figure 22

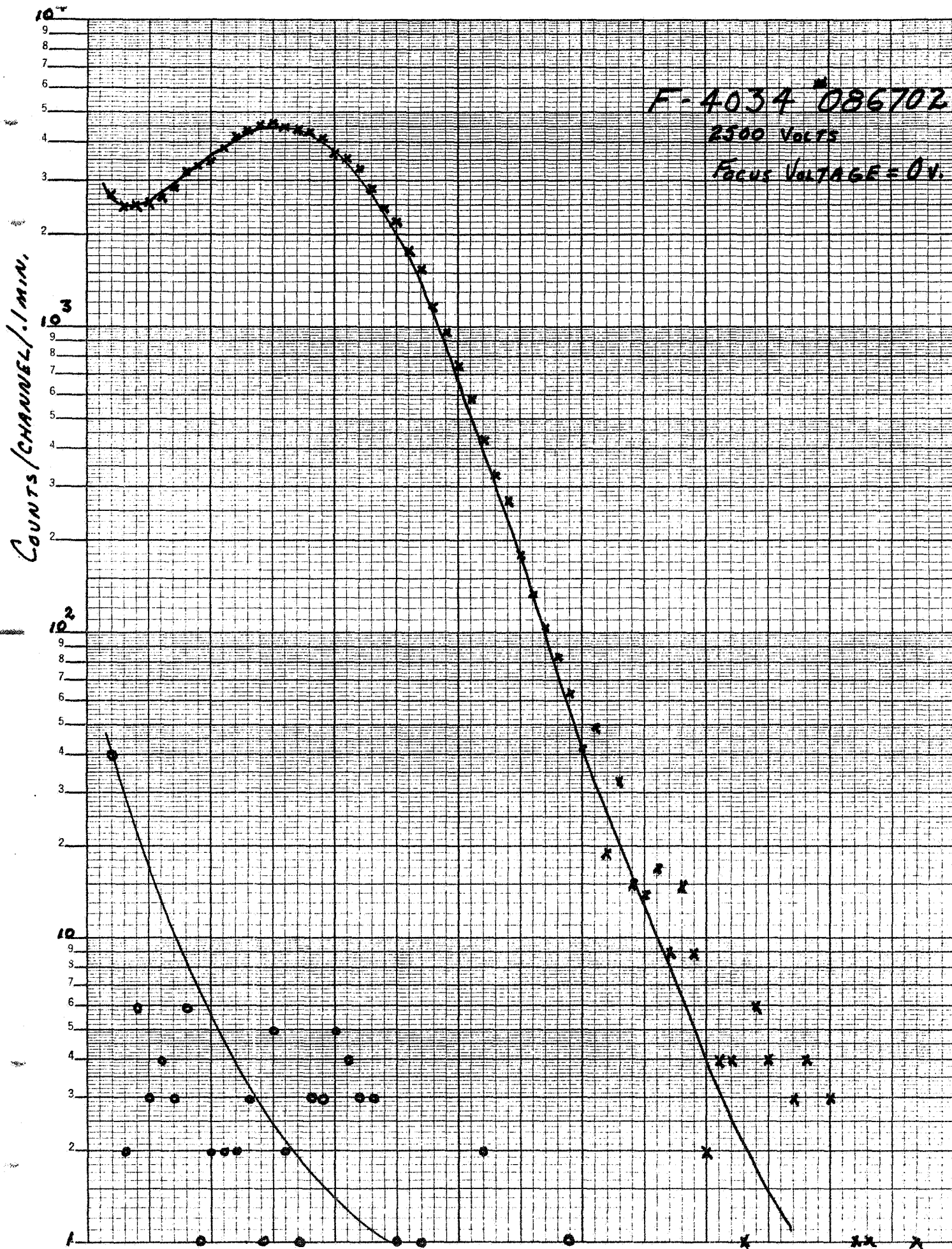
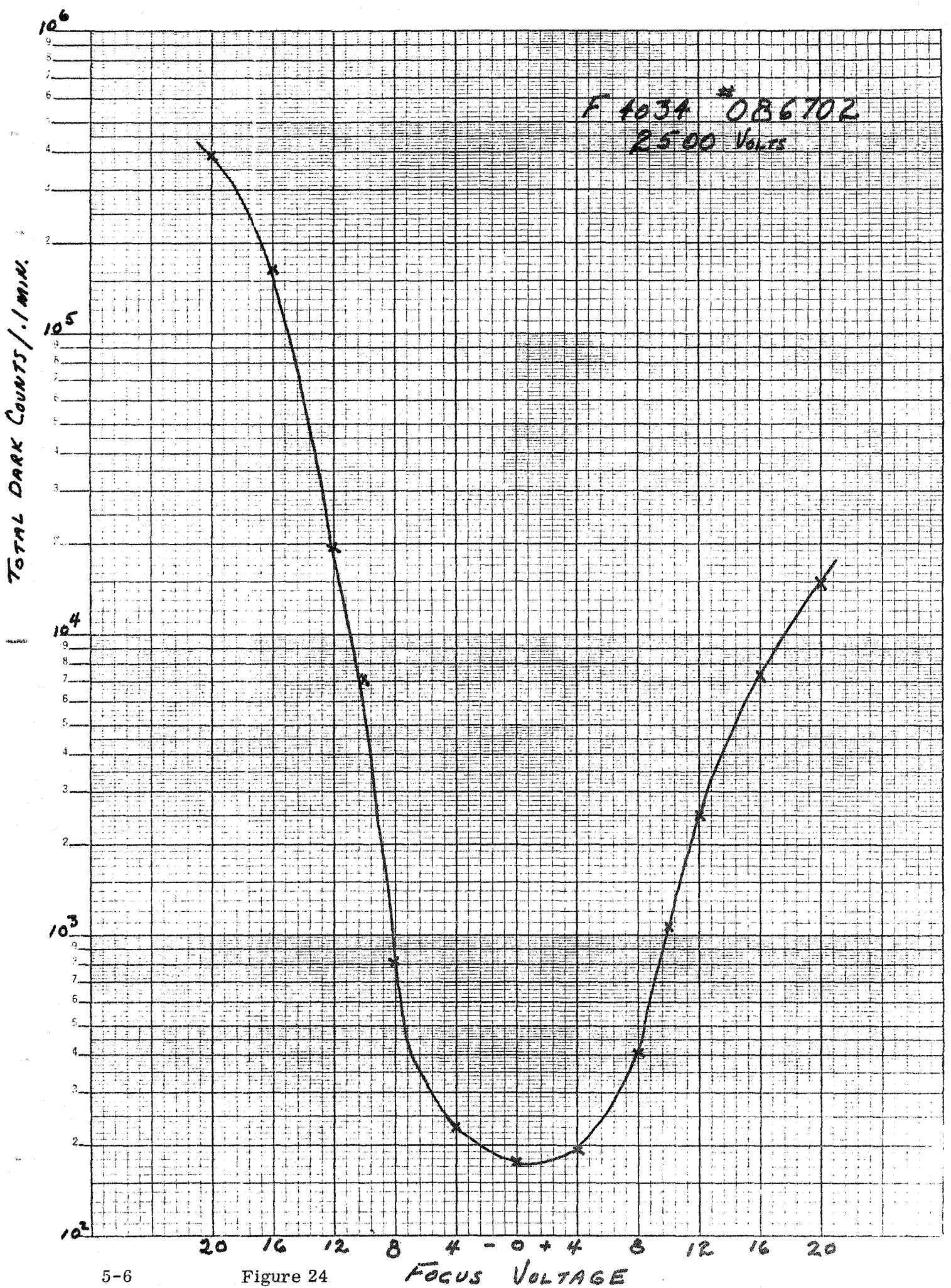


Figure 23



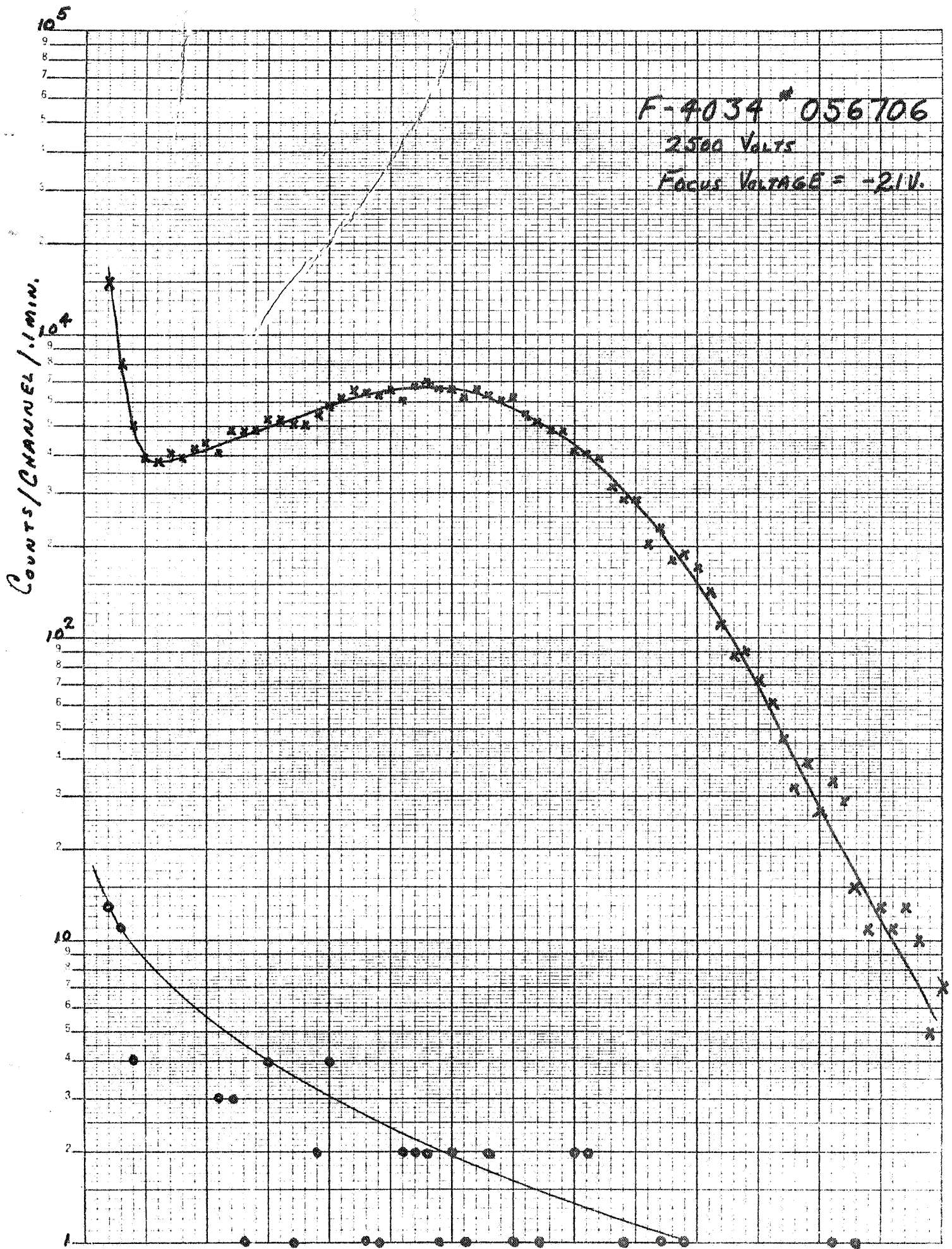
the gap between cathode and focus electrode a discharge is produced which emits electrons that find their way into the multiplier. Such a discharge is not difficult to explain since the two electrodes are formed from a hickel evaporation on the glass wall of the tube. This evaporation is cut by a fine high pressure jet containing an abrasive. This "ragged" cut may act as a sponge for alkali metal vapors which might further compound the difficulty.

The fact that the dark count is higher for a negative potential must certainly be due to the fact that photon and thermionic electrons are emitted from the cathode materials deposited on the focus electrode, an inevitable consequence of the photocathode formation process. These electrons would, of course, be suppressed when positive potentials are applied to the focus electrode.

Following the tests described above, some further tests on Tube No. 056706 were performed to determine what might account for the differences in the focus characteristics of the two tubes. It was discovered that there is a serious unstable leakage internal to the tube which causes the potential difference between cathode and focus electrode to vary widely. This was first noted when the anode response was being remeasured and the output was observed to fall off slowly. Subsequent observation of this change with a meter connected to focus electrode showed voltage excursions of as much as 10 to 15 volts. Since no means for continuously monitoring this potential is provided in the pulse counting equipment, it would appear that the low dark counting rate and good signal distribution shown in Figure 25 for Tube No. 056706 might well be due to a change in the focus electrode potential. The foregoing data seems to indicate that the focusable image section in these tubes does indeed contribute to the dark counting rate. It is interesting to note, however, that the tube described is capable of good statistics notwithstanding the lack of optimum focus potential, a fact already demonstrated by the premium performance of the FW series of ITTIL multipliers.

5.2 Windowless Multipliers

A second tube type tested was the 16-stage multiplier designated F4074. This device is intended to be used in such applications as the short wavelength radiation detectors or in mass spectrometers where ions impinge directly on the secondary emitting surface of dynode one. Structurally, these multipliers have the voltage divider supported directly on the multiplier assembly so that the only connections required are to the high voltage supply and an appropriate anode output signal lead to a meter or counting circuit. The particular unit tested was a modified version of the standard F4036 in that the dynode support plates were spaced so that the ends of the dynodes are approximately 1/8 inch away from these insulator surfaces. This was done to reduce the possibility of stray electrons reaching the insulator surfaces and producing charge patterns that would further distort the electron trajectories and produce additional stray electrons. In addition, the fine wire grids used in front of



the dynodes were replaced by photographically etched nichrome mesh. The dynode material remains unchanged; namely beryllium copper, and the same type resistors, 1 megohm 1/4 watt glass enclosed resistors are used for the voltage divider. The fully guarded anode structure is also maintained. This consists of a glass filled eyelet through which a wire is sealed to act as both a support and lead for the anode. The eyelet body and a tab protrudes through the dynode support plate and the tab is welded to the ground terminal of the voltage divider.

Figure 26 is a photograph of this multiplier removed from its evacuated glass shipping container.

The tests to be described were made with the tube mounted upright in a shielded enclosure, high negative potential applied to dynode one, and the entrance aperture. The anode could be connected either to a microammeter or to a pulse amplifier for pulse counting. Since a 9741 glass window is used in the end of the envelope, it is possible to use a UV light source to excite dynode one as a photocathode. The light sources used for this purpose was a low pressure mercury discharge lamp in a quartz envelope (Pen-Ray Model 11 SC-1A) with its output largely at 253.7 nanometers.

Measurements show this multiplier to have a gain of 1.5×10^6 at 2600 volts and a dark current of 3.2×10^{-12} . Gain measurements are performed with an electrometer in dynode one lead to measure D1 output current and a microammeter in the anode lead.

There is, however, a difficulty which has not yet been resolved with regard to determining dynode one current. It does not seem to be possible to change the overall voltage, for the purpose of obtaining a gain curve, without changing dynode one current even though the light input is held constant. A saturation curve was plotted using the aperture as collector. The results were quite predictable with complete saturation occurring at about 60 volts. This, however, is not the normal mode of operation but a special tube will be required with a lead from dynode two available to obtain this data with dynode two as the collector.

The statistics of the multiplier when excited with UV radiation of the wavelength mentioned above are shown in Figure 27. A peak-to-valley ratio of 1.2 was obtained with a total dark count of 7 per second. The positioning of the light over dynode one is quite critical and the intensity must be reduced by means of several thin glass cover slides or pieces of cellophane. It is also essential that an aperture be used to confine the input radiation to a restricted area of the first dynode.

Failure to observe these precautions can result in the complete loss of the Poisson type statistics shown in Figure 27 and an exponential distribution will result. These facts indicate again the critical nature of the region about dynode one with regard to the ability of a multiplier to function as a single event counter.

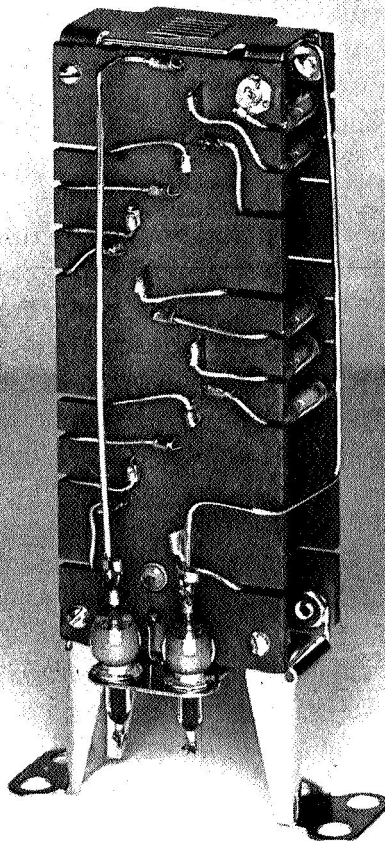


Figure 26 F4074

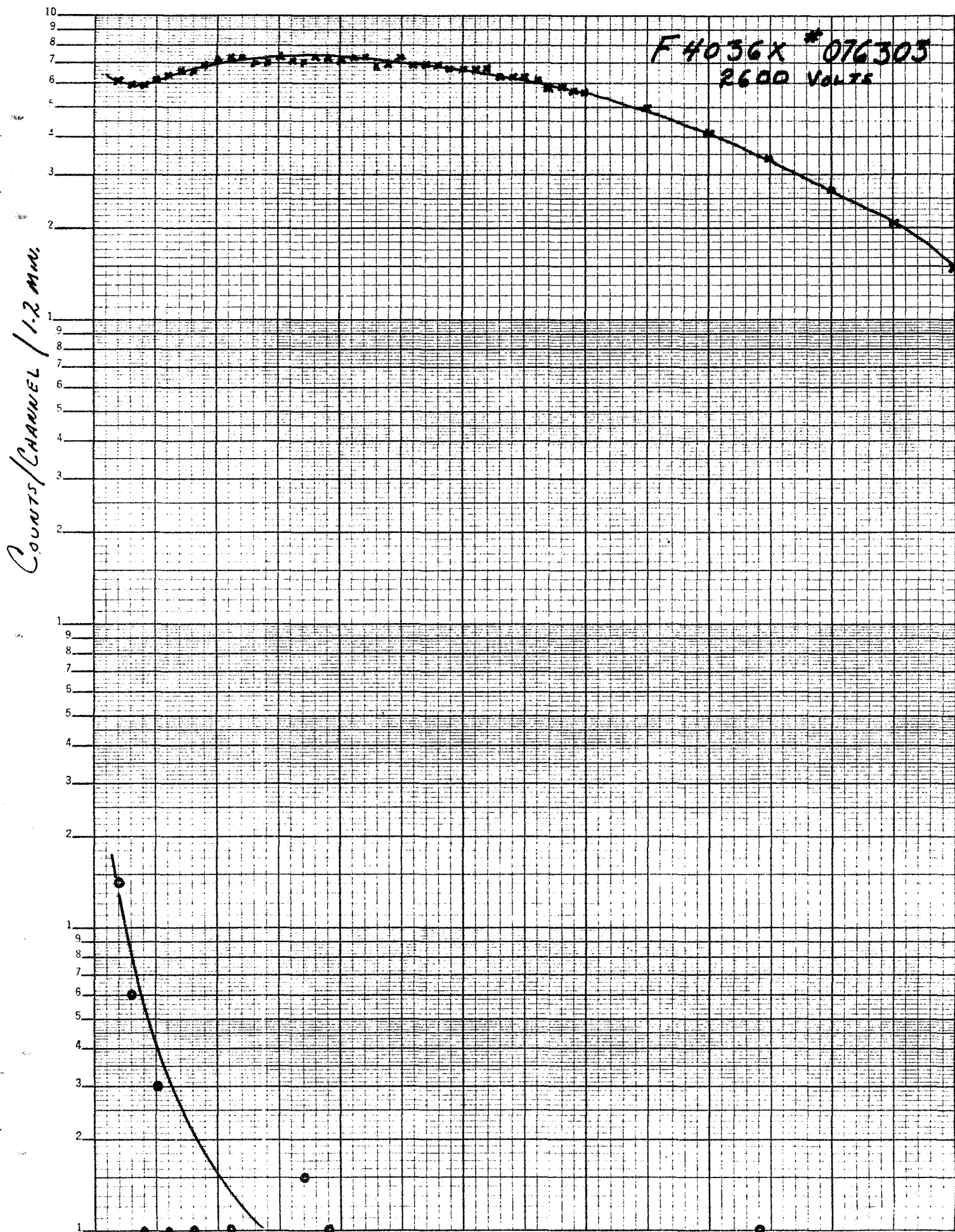


Figure 27

5.3 Multiplier Phototubes with Remotely Processed Cathodes

Perhaps the most promising approach to producing an improved multiplier phototube is the processing of the photocathode before sealing it to the tube envelope. This results in a clean, cesium free tube interior and freedom from the problems associated with this contamination. Cesium of the multiplier may produce some contamination of the tube interior though this process allows more rapid removal of excess cesium than the standard process. It also provides an opportunity to form a group of cathodes, and select the best for the tube under construction.

While neither the technique nor the equipment for accomplishing this task were developed on this project, it seemed appropriate to adapt the process, developed at ITTIL, to a particular tube geometry which is suitable for astronomical detection purposes. The two major requirements are small tube diameter, 1 inch or less, and as large an effective photocathode, in that diameter, as possible.

The F4075, see Figure 28, is 1 inch in diameter, has a standard JEDEC 13-B, 13 pin stem and the possibility exists that a 0.5 inch diameter cathode, can be obtained while maintaining the unique features of the ITTIL multiplier phototube image section design. This latter qualification will require the development of an image section with a magnification of 0.1, to be used in place of the present designs which have a magnification of 0.7 or 0.4.

Four tubes of this type have been built, the first of which was a leaker and was subsequently disassembled. The other three have been tested though one had a cathode of low sensitivity due to defective alkali metal generator. This tube functioned so poorly that test data was not obtainable.

Each tube has a fused silica entrance window on which the photocathode is formed. This type of faceplate gives UV response and minimizes sensitivity to high energy particle bombardment. The electron multiplier is a 16 stage device with a voltage divider between dynode three and twelve welded directly to the dynode tube on the multiplier support plates.

The inclusion of a portion of the divider in the envelope allows the use of the standard 16 stage multiplier in a 1 inch blank with a 13 pin stem.

The photocathode of these tubes conforms closely to the S25 response shown in Figure 29.

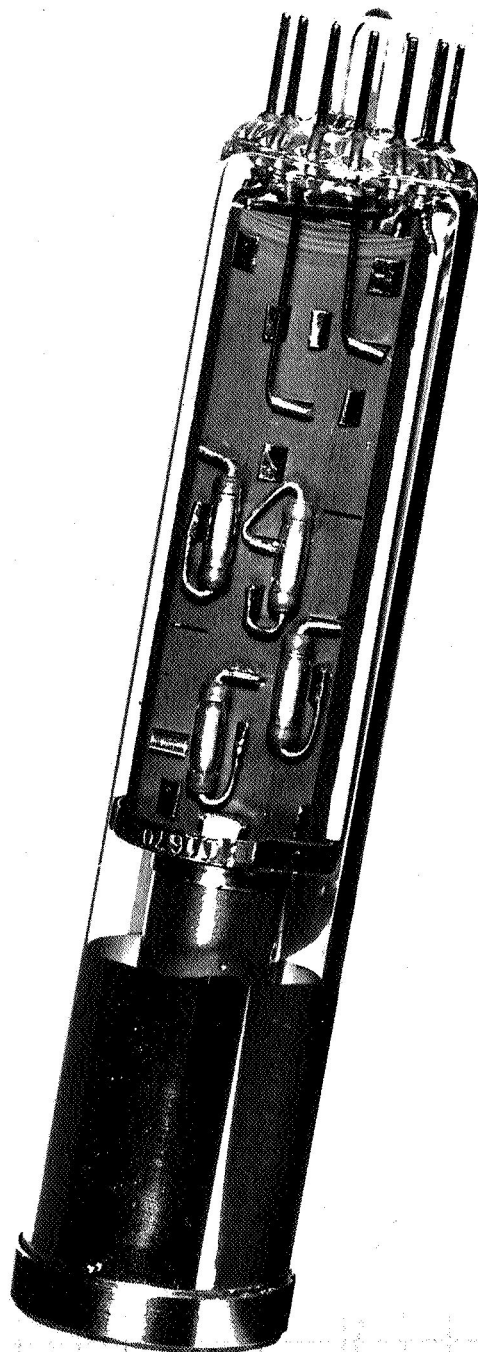


Figure 28 F4075 Multiplier Phototube

TYPICAL ABSOLUTE SPECTRAL RESPONSE CHARACTERISTICS

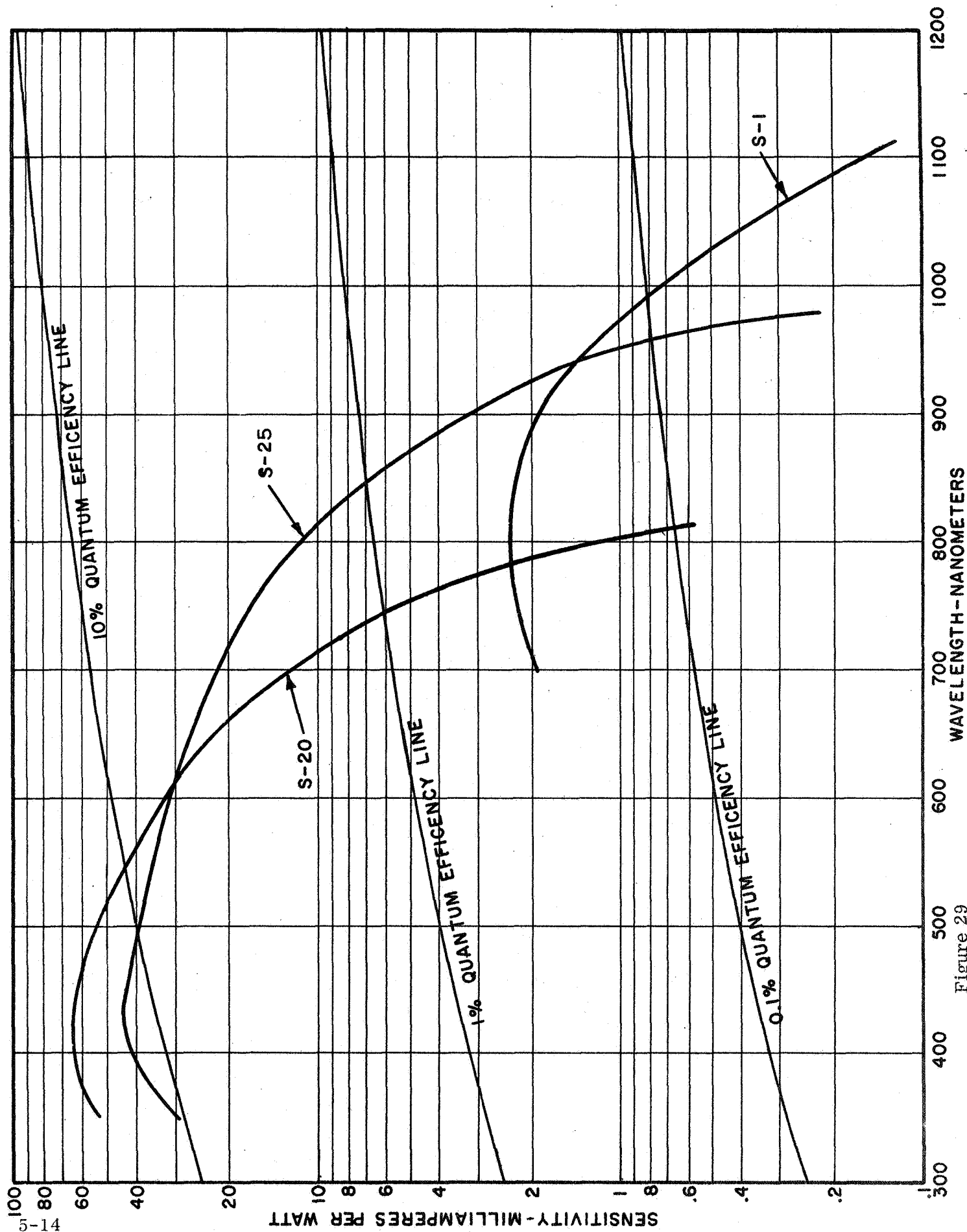


Figure 29

The obvious advantage of increased quantum efficiency of the S25 photocathode between 800 and 950 nanometers, with only minimal decrease in peak quantum efficiency, is accompanied by increased life at a given cathode current density, a higher peak output current without field distortion or defocusing, thermionic dark noise comparable to the S20 cathode and it is adaptable to multiple reflection optical trapping for further QE enhancement.

Figures 30, 31, and 32 are the spectral response curves for F4075 106702, 116701, and 116702 respectively. In Figure 29 the crosses indicate the effect of cooling to -30 degrees C. It is expected that even closer agreement with the typical S25 curve will be obtained when more samples of this type tube have been constructed and processing techniques have been refined. However there does exist a potential difficulty associated with the quartz faceplate. Quartz is known to be semi-permeable to helium and the leak rate ratio of quartz as compared to 7052 (borosilicate) glass is about 100 times.

A test program has been initiated in this laboratory to investigate the effect of helium diffusion on tubes in standard 7052 glass envelopes, stored in a helium atmosphere. However, it is not certain that significant results were forthcoming during the course of this contract.

Several tubes with quartz envelopes, which have been on the shelf 2-1/2 years were tested to determine if their characteristics had deteriorated. No evidence could be found that they were in any way less sensitive or more noisy than they were when built. This would seem to indicate that helium diffusion should not impose serious limitations on the life of such tubes but quantitative data is not available now to substantiate such a conclusion.

Figures 33 and 34 are the d-c characteristics for tube numbers 106701 and 116702. Both tubes have similar gains, the dark current curves, however, have very dissimilar slopes indicating that the dark current for 106702 is primarily ohmic leakage which is not affected by the gain of the multiplier. Figures 35 and 36 are the pulse height distribution for the same two tubes; the upper curves are the signal plus dark count distributions and the lower curves are dark counts only. Both tubes have good peak to valley ratios of about 2.

The lower dark count for 106702 is due to its smaller effective photocathode area, which is approximately one tenth that of 116701.

Both of these tubes have been consigned to Lick Observatory, where they will be considered for use as cooled detectors in photon counting applications. Tubes previously built for this purpose and reported on an earlier⁹ contract exhibited

9 Final Report - Research in the Development of an Improved Multiplier Phototube Contract NASw 1038, November 16, 1966.

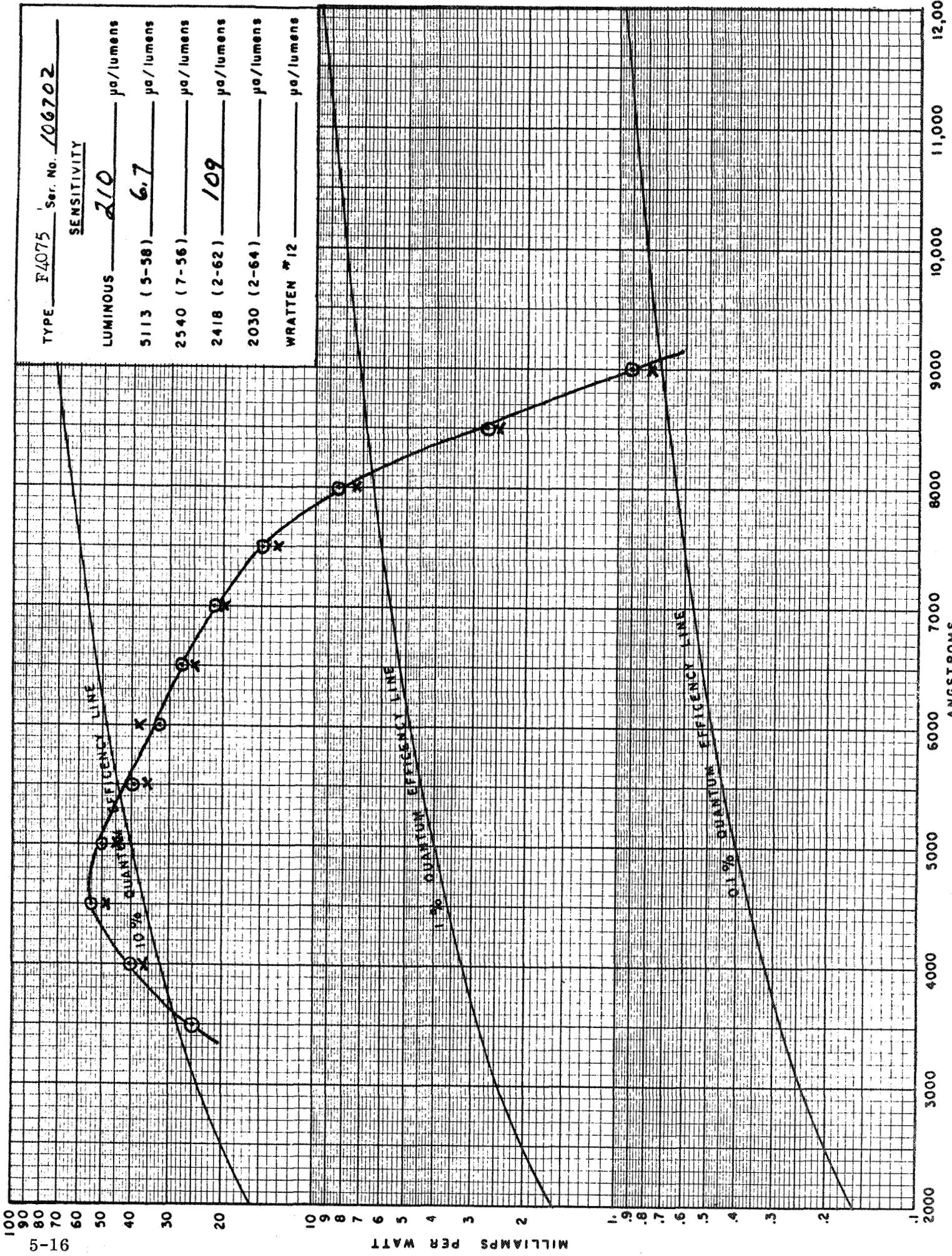


Figure 30

TYPE F4075 Ser. No. 116701

SENSITIVITY

LUMINOUS 155 $\mu\text{a/lumens}$

5113 (5-58) 5.4 $\mu\text{a/lumens}$

2540 (7-56) $\mu\text{a/lumens}$

2416 (2-62) 80 $\mu\text{a/lumens}$

2030 (2-64) $\mu\text{a/lumens}$

WRATTEN #12 $\mu\text{a/lumens}$

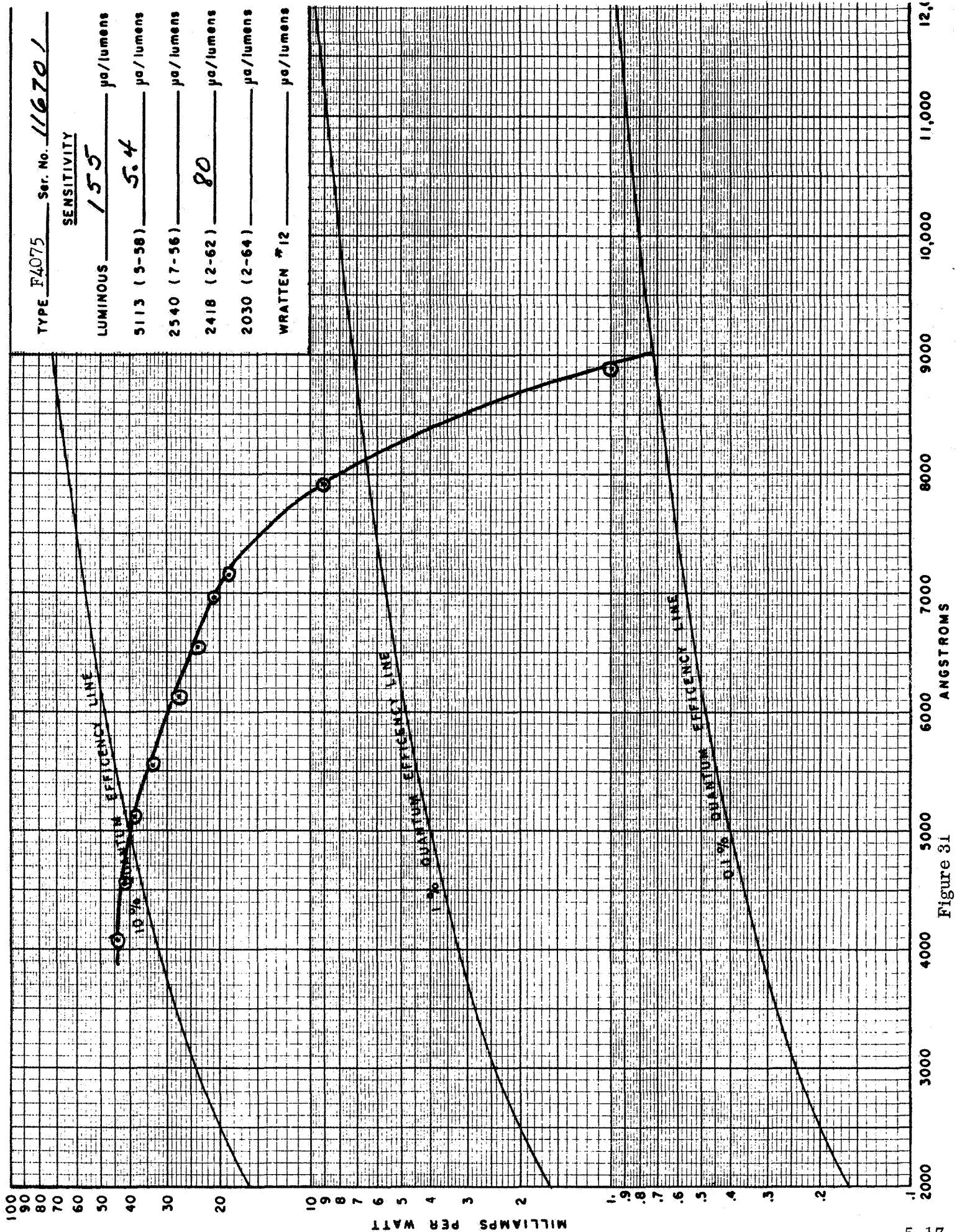


Figure 31

TYPE F4075 Ser. No. 116702

SENSITIVITY

LUMINOUS 59 $\mu\text{e/lumens}$

5113 (5-58) 4.1 $\mu\text{e/lumens}$

2540 (7-56) $\mu\text{e/lumens}$

2418 (2-62) 20 $\mu\text{e/lumens}$

2030 (2-64) $\mu\text{e/lumens}$

WRATTEN #12 $\mu\text{e/lumens}$

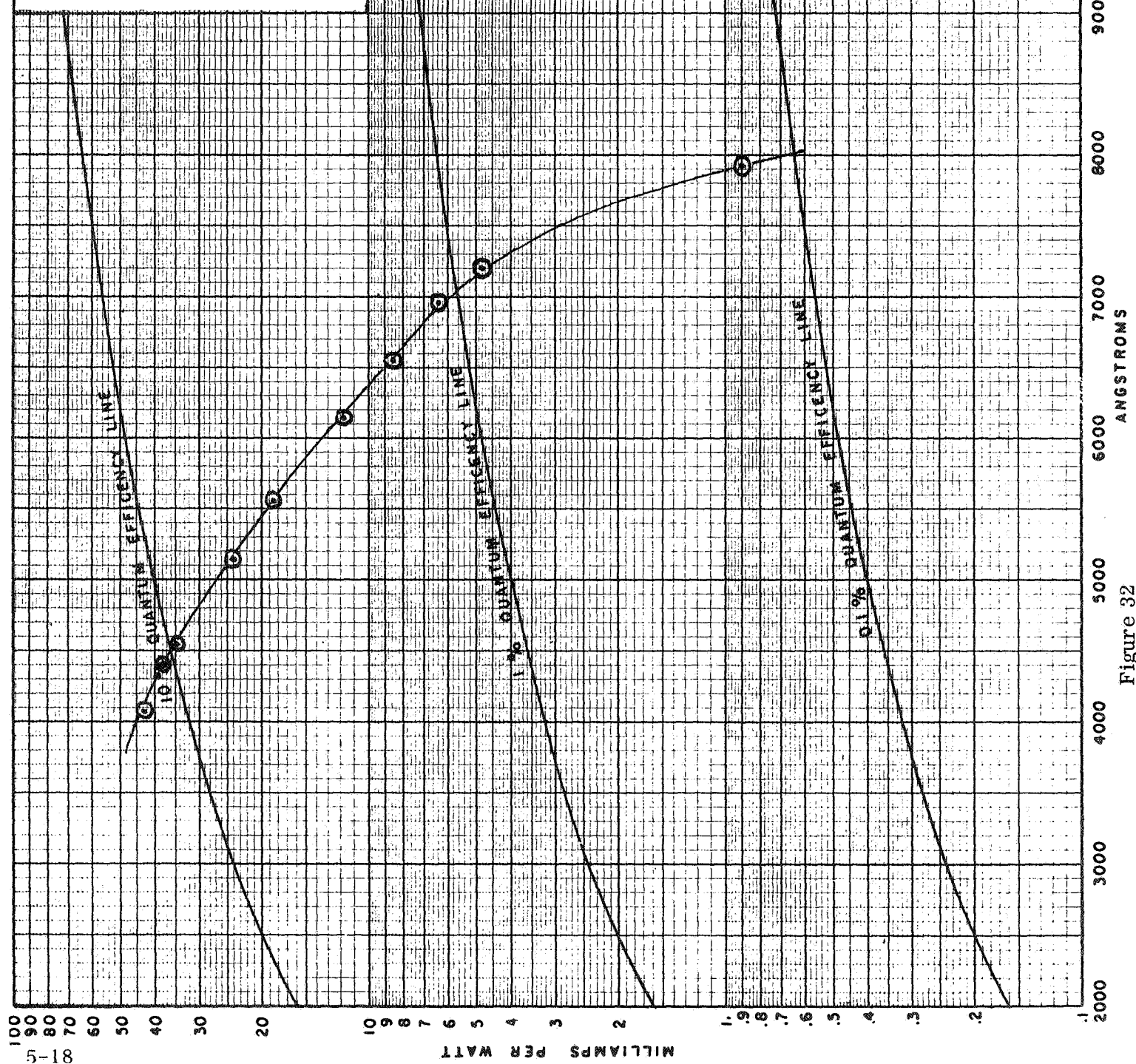


Figure 32

ANODE RESPONSE (AMPERES/LUMEN)

F4075
116701 (350 LEPD)

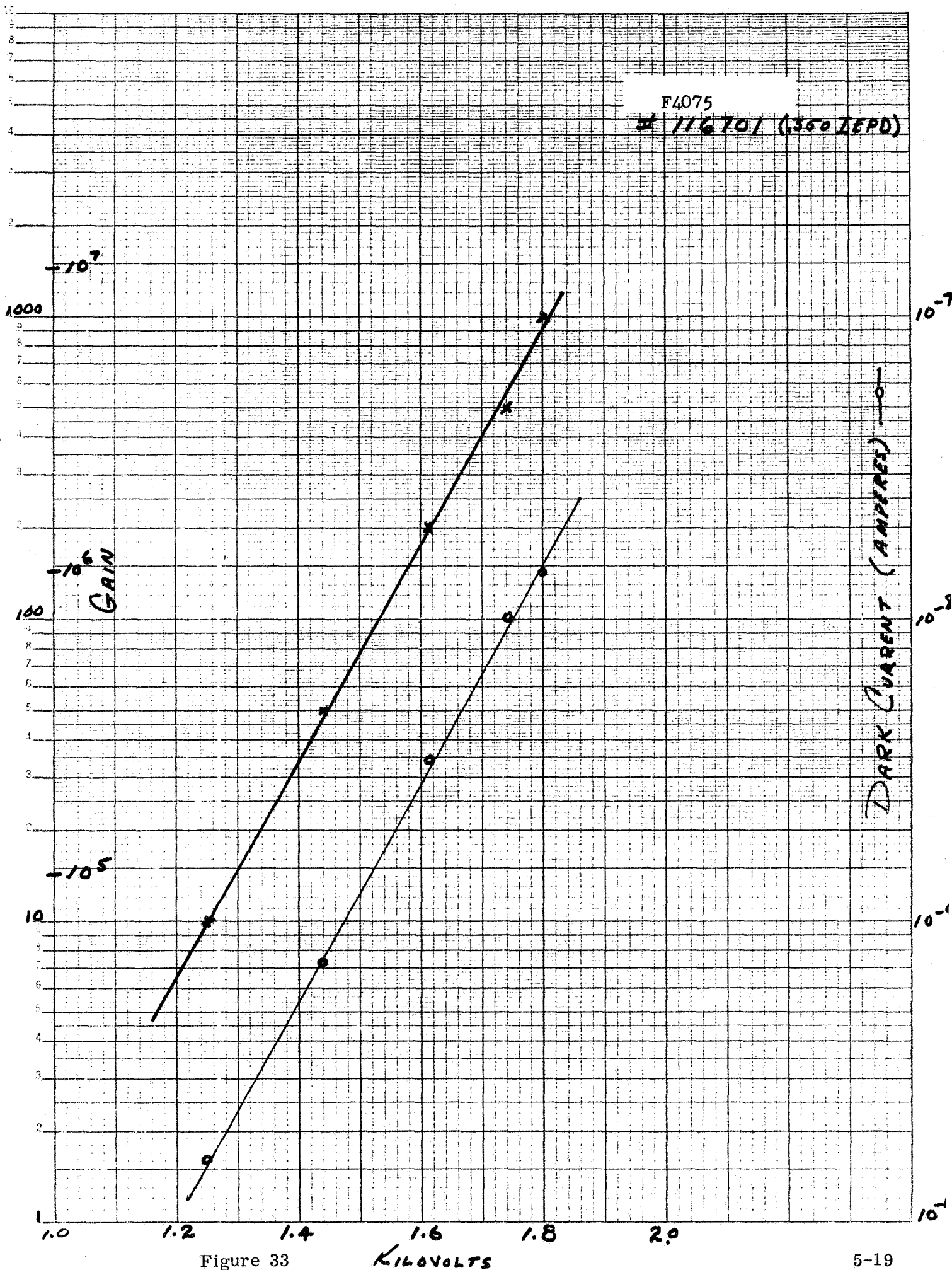


Figure 33

KILOVOLTS

ANODE RESPONSE (AMPS/LUMEN)
 GAIN

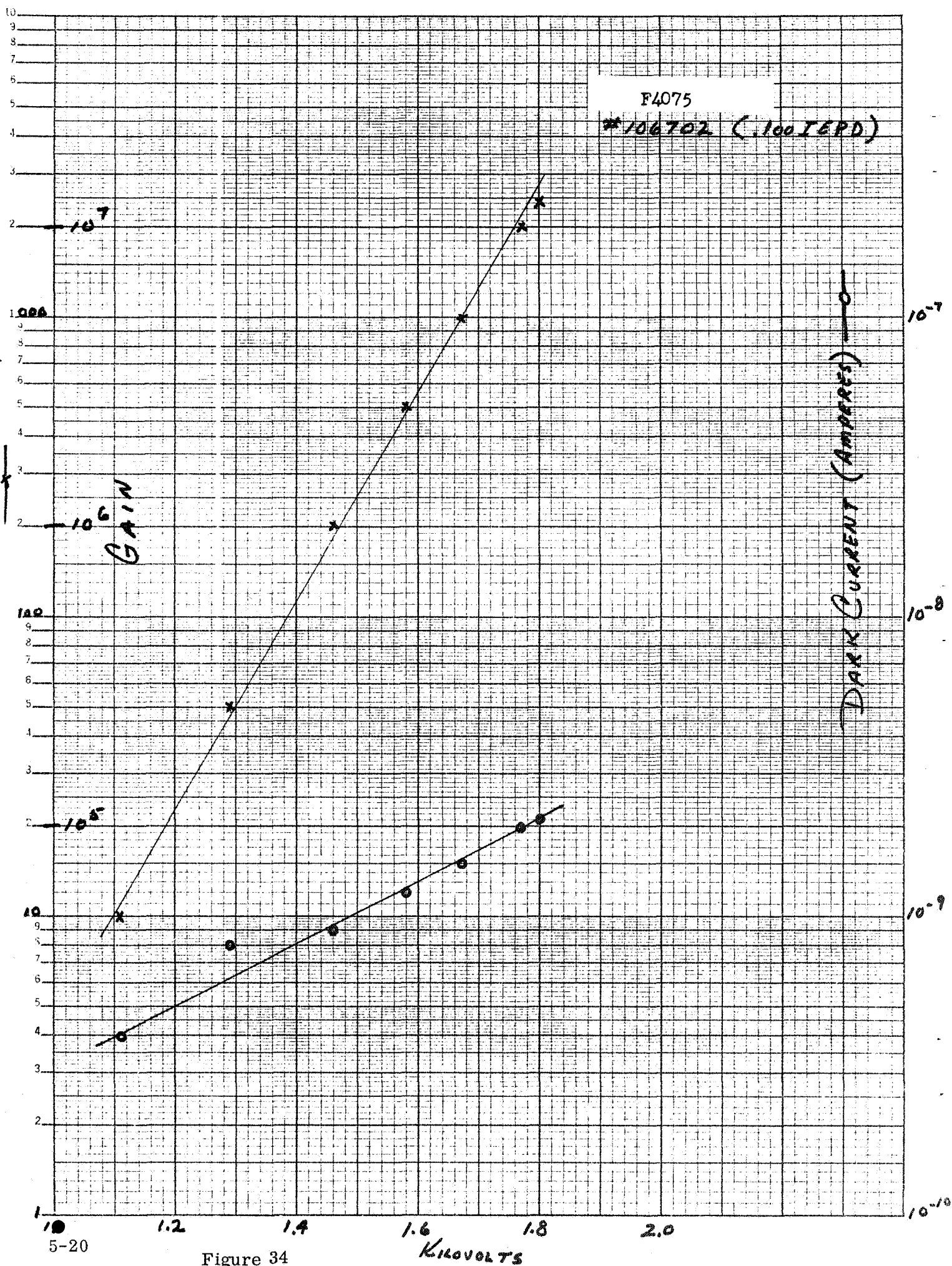


Figure 34

COUNTS/.MIN/CHANNEL

46 6013
SEMILOGARITHMIC
PLOT OF COUNTS/.MIN/CHANNEL
VS. CHANNEL NUMBER

I4075
*116701 (.3501EPD)

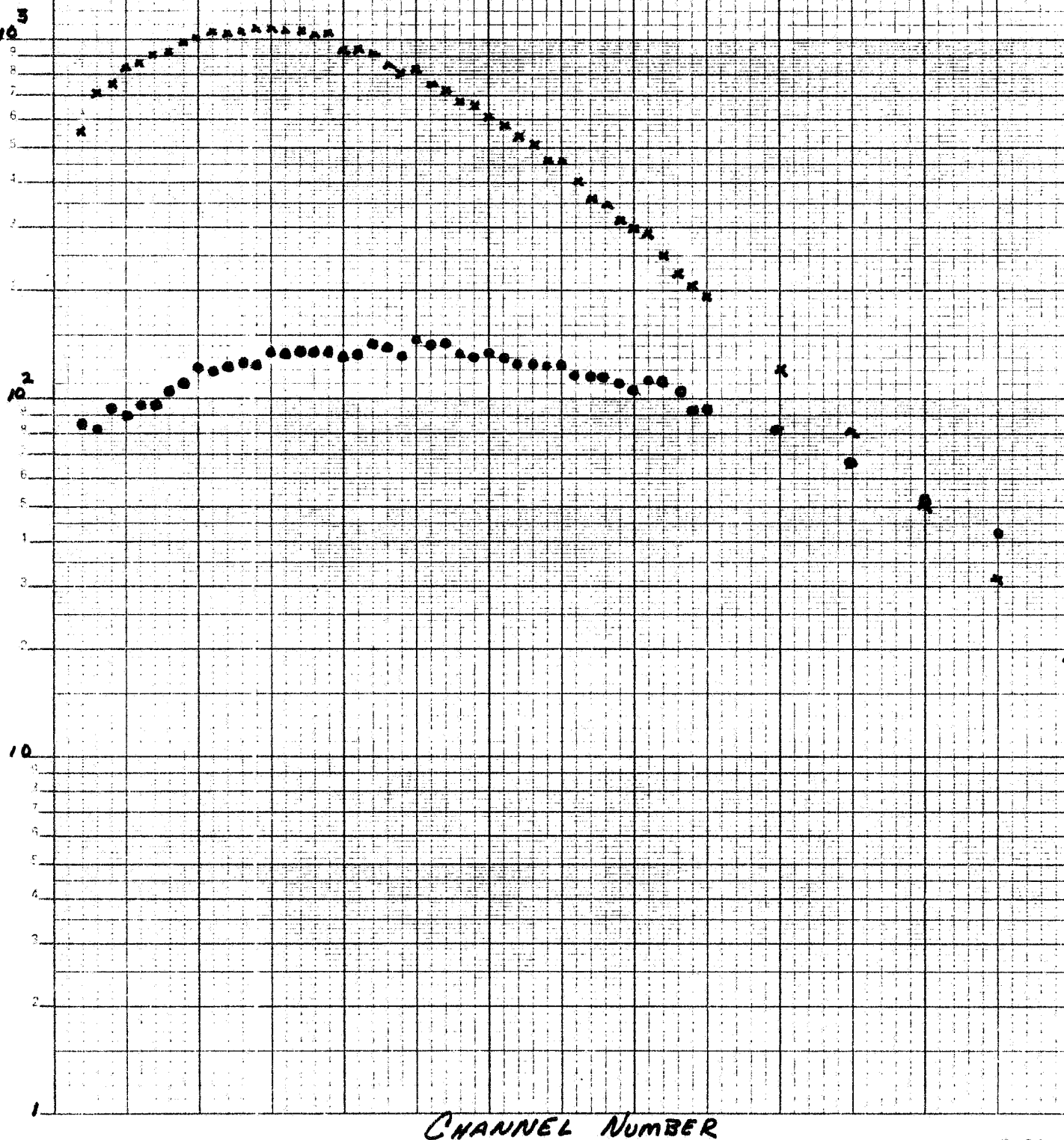
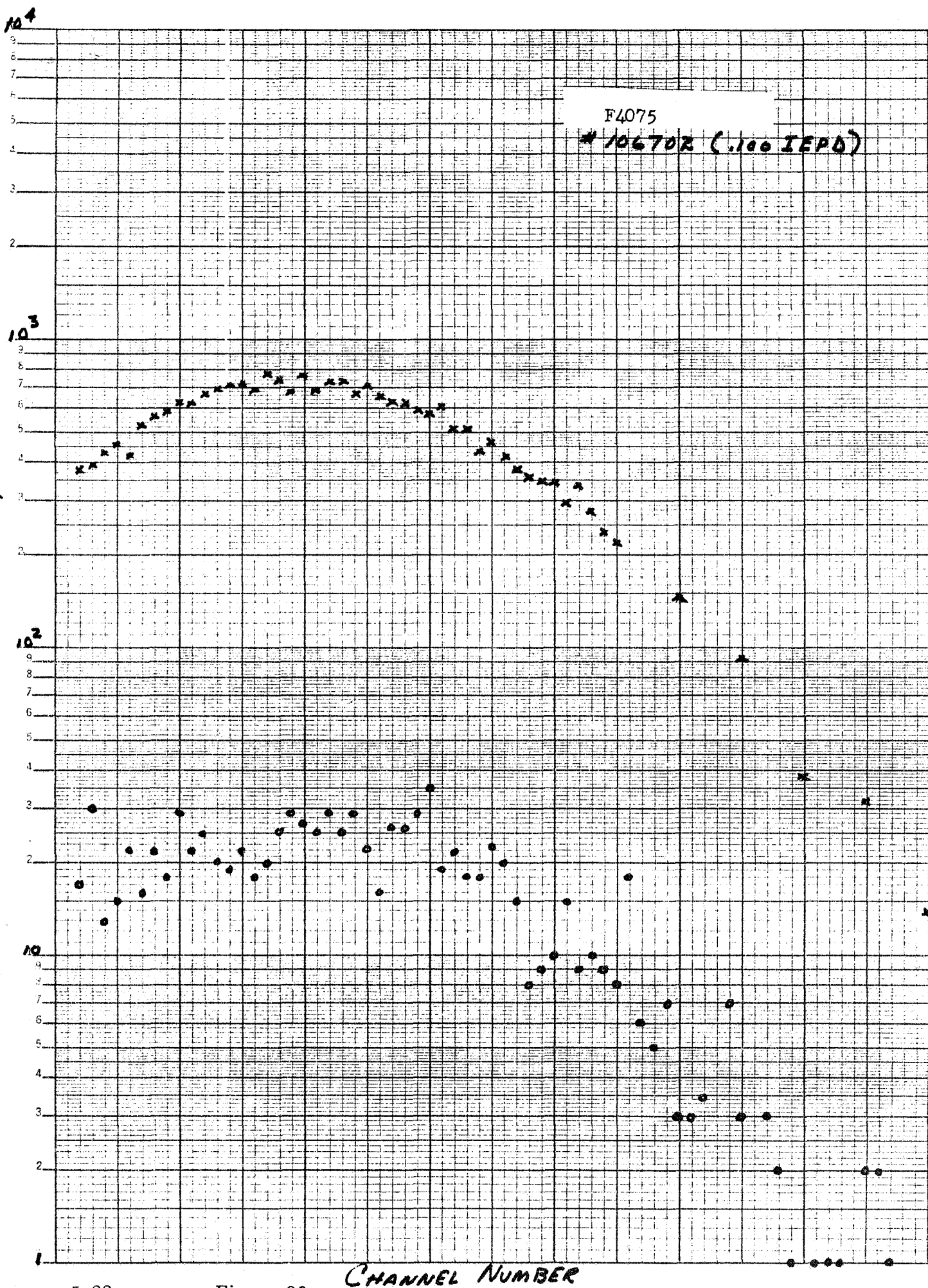


Figure 35

COUNTS/.1 MIN. / CHANNEL



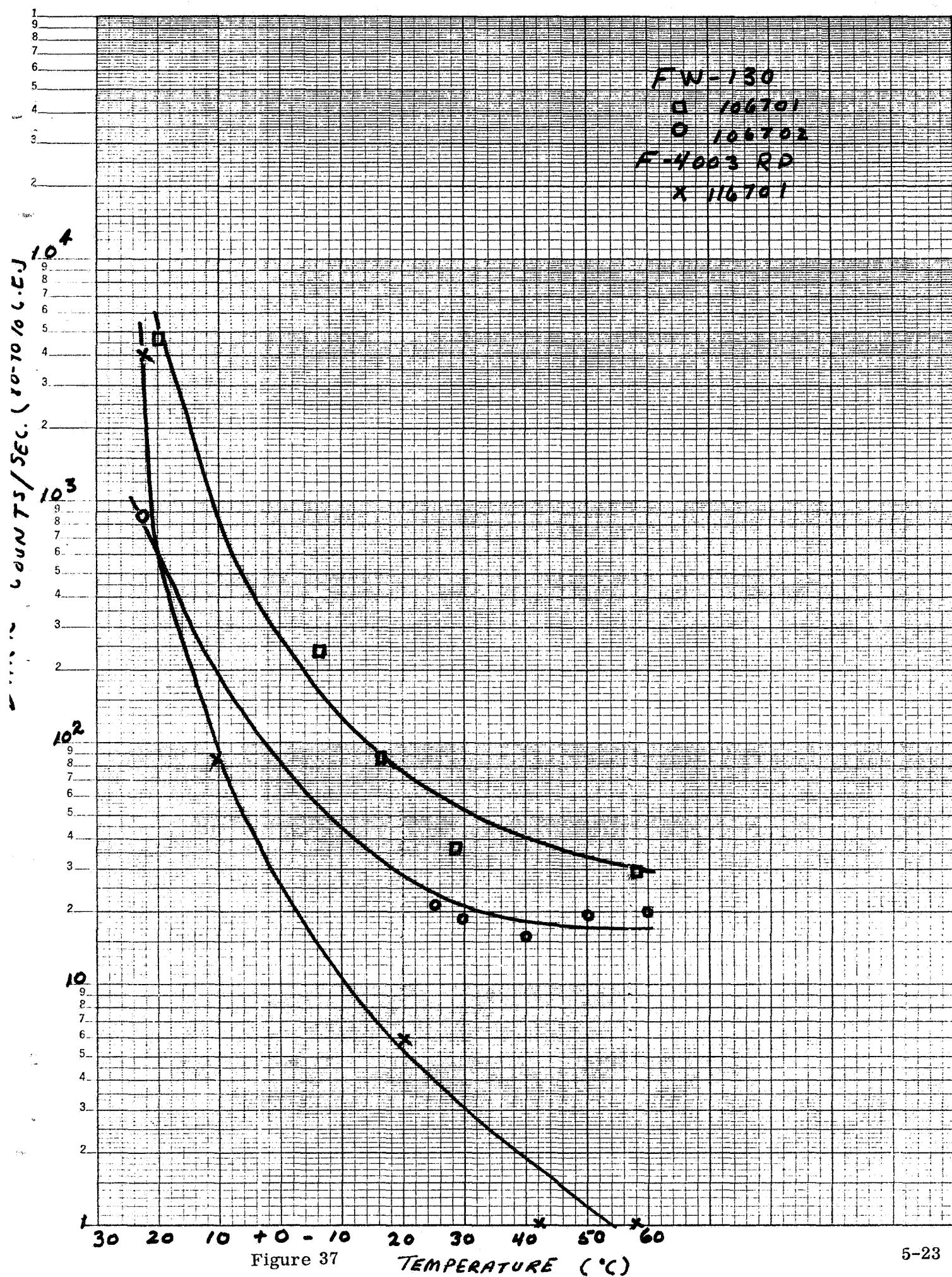


Figure 37

occasional pulses of large amplitude which, in our equipment, appeared to be equal to many electrons. In the equipment at Lick Observatory, however, these pulses were resolved into their component single electron pulses because of the high resolution pulse processing circuits. This behavior is objectionable, especially at low counting rates. Though this difficulty does exist to a certain degree in all glass tubes, a large portion of this problem was found to result from the use of sapphire windows to extend the cathode response into the UV.

Tests showed that sapphire (ultrapure Al_2O_3) is an efficient scintillator which is easily activated by cosmic radiation and residual radioactivity in the tube itself and the local environment.

Preliminary test at Lick shows the first of these new tubes (0.100 inch IEPD) to be comparatively free of these multiple-electron pulses. The second tube (0.350 IEPD) is still being evaluated.

Cooled data was taken on only one of these tubes after the tube cooler was modified. Earlier data was unreliable due to poor temperature control and lack of thermal contact with the tube envelope.

This new tube type lacks one desirable feature of the standard FW130 design in that the aperture electrode is now sealed into the glass envelope thereby interposing a light stop between the photocathode and the multiplier section of the tube. Whether or not this fact will detract from the operation of the tube is not yet known and any decision as to the advisability of a design change in the F4075 to include this feature will depend on the results of further evaluation.

6.0 ANALYSIS OF STANDARD ITTIL MULTIPLIER PHOTOTUBE DATA

The objectives of this data compilation and study were the determination, and comparison of ITTIL FW130 characteristic parameter values in analog (dc) and digital (single - electron¹⁰ pulse count) modes of information processing. A companion purpose was the reappraisal of tube specifications pertaining to these characteristics. The procedure followed was tabulation of available data on a large sample of FW130 tubes, with rejection of data on tubes for which only d-c data was available but retention of data whenever pulse-counting had been attempted even if performance had been unsatisfactory in the pulse counting mode.

The collected data appears as Table V. Cathode sensitivity was measured with the tube in a diode configuration; all other parameters were measured at the anode, with standard divider potentials. The d-c parameters (anode dark current, operating voltage, and equivalent noise input) were recorded for a constant anode responsivity of 2000 amperes per lumen. Other parameters were recorded for the designated operating voltage or responsivity at which data was available. Three dark current measurements appear in Table V and require explanation. The first and third are the usual dark current at 1800 volts and 2000 amperes per lumen respectively; the second, "@1800 volts K@D2", denotes a dark measurement made at 1800 volts with the cathode raised to the potential of the second dynode. This potential is positive with respect to the first dynode, and the dark current so measured is an indication of leakage across the stem and dynode thermionic emission.

Pulse count data had been determined at a common 1800 volts, but is readily compared to its d-c counterparts as the number of significant pulses is not generally voltage sensitive. "Total pulses per second" is the number above a small and undetermined bias level; this parameter is voltage sensitive and not very significant. The "80 to 90 percent C. Eff. "pulses per second are those measured with a pulse-height bias level adjusted so that approximately 85 percent of the single electron pulses¹⁰ are counted. The proper bias level is determined for each tube from its differential pulse height distribution with a light input. It is set at 60 percent of the peak. "Total pulses K@D2" should be analogous to the corresponding dark current. This information, however, is useful only qualitatively as it is measured at the undetermined bias level. The "peak to valley ratio" is of the light input differential pulse height spectrum. A criteria used requiring at least a peak-to-valley ratio 1.1:1.0 to set the 80 to 90 percent bias level provides assurance that the tube is operating properly.

10 The term "single electron" used herein refers to the triggering charge input to the first dynode. All countable output pulses contain many electrons, normally between 10^6 and 10^8 .

Table V

IEPD Diameter: .254 cm (.100 in.) Area = .0506 cm²

Tube Number	Cathode Sens. $\mu\text{a}/\text{l}$ 2870°K W	Operating Voltage @2000a/l	Dark Current (amps $\times 10^{-10}$)			Equivalent Noise Input lumen $\times 10^{-14}$	Dark Pulses/Second ^d			Peak-to-Valley Ratio	Noise Factor @200 a/l	Single Electron Pulses	
			@1800V	K@D2 @1800V	@2000a/l		Total	@80-90% C. Eff.	K@D2*			Per Cm ² Equivalent	Per Second Measured
1	160	1980	0.03		0.08	5.3	62	45		1.2			
2	115	1740	3		3	< 5.3	45	40		1.5			
3	175	1730	3	1.4	3	< 3.5	950			1.08			
4	147	1890	24	24	26	< 5.3	15000	31		1.3			
5	192	1700	1.7		1.7	< 5.3	96	31		1.2			
6	192	2050	0.1		1.1	6.3	105	83		1.3			
7	184	1710	10	1.3	4.6	4.2	8625			Exp.			
8	103	1860	2.4	1.1	3.1	4.2	81	59		1.2			
9	120	1690	5.5		2.5	< 3.5	21	7		1.2			
10	144	1900	3.6	2.6	6.2	< 4.6	31	25		1.1			
11	196	1820	2.8	0.4	2.8	< 3.5	262	67	2	1.4			
12	214	1710	5	3.1	5	< 3.5							
13	200	1750	84	42	70	10.9	30000			Exp.			
14	195	1810	2.3	0.11	2.5	3.5	294	11	3	1.1			
15	148	2060	1.1	64	3	3.5	111	53		1.6			
16	137	1780	18	0.68	15	9.8	463	300		1.4			
17	149	1880	115	110	125	13.4	196	90	5	1.5			
18	158	1850	12	2.7	12	10.9	105	87	0	1.3			
19	157	1780	220	210	210	4.6	154	98		2.2			
20	143	1980	2.2	1.1	6.4	5.3	143	44	0	1.1			
21	245	1770	22	4.4	16	9.9	689	226		1.2			
22	170	1780	2.7	1.8	2.4	3.9	761			Exp.			
23	216	1710	10	3.3	4.1	5.3	219	93	96	1.5			
24	135	1910	6.8	5.9	14	8.1	17000			Exp.			
25	180	1850	1.7	0.6	2.2	6.3	217	150	11	2.0			
26	180	1670	22	13.5	8.4	4.9	1202	74	526	1.2			
27	200	1570	60	2.2	9.4	7.0	248	16	72	1.4			
28	176	2080	1.3	0.67	3.3	7.04	385	23	127	1.4			
29	140	2070	15	14.5	22	6.3	58	19	29	1.6			
30	140	1950	12	1.6	36	24	291	172	42	1.5			
31	179	1750	24	2.6	16	< 3.5	201	99	18	2.0			
32	123	1710	15	5	7.1	5.60	509	31	462	1.6			
33	120	1960	8	7.0	12	6.0	74	16	66	2.0			
34	195	1840	12	4.6	16	9.16	1344	282	90	1.5			
35	168	1850	40	38	52	8.1	300	38	118	1.2			
36	175	1960	7.5	2.6	20	13.0	153	82	42	1.9			
37	178	2430	0.16	0.05	1.2	< 3.5	184	77	3	1.2			
38	145	1780	10	3.0	7.6	6.33	179	100	17	1.4			
39	186	2020	4.2	0.05	14	13.4	240	169	10	1.4			
40	164	1770	4.4	3.2	4.4	4.57		16	28	1.7			
41	171	1910	24	22	50	8.1	183	55	154	1.4			

Table V (Continued)

IEPD Diameter: 0.360 cm (0.140 in) Area = 0.100 cm²

Tube Number	Cathode Sens. $\mu\text{a/l}$ 2870°K W	Operating Voltage @2000a/l	Dark Current (amps x 10 ⁻¹⁰)			Equivalent Noise Input lumen x 10 ⁻¹⁴	Dark Pulses/Second		Peak-to-Valley Ratio	Noise Factor @200 a/l	Single Electron Pulses	
			@1800V	K@D2 @1800V	@2000a/l		Total	@80-90% C. Eff.			Equivalent	Per Second Measured
1	202	1640	70	47	53	4.9	152	109	1.5		1100 x 10 ¹	109 x 10 ¹
2	120	1710	13	0.8	6.6	6.3	246	163	1.4	1.4	230	163
3	184	1760	3.6	2.1	2.9	< 2	444	263	1.1	1.46	64	263
4	165	1870	110	89	110	21	1460	132	1.2	2.76	1080	132
5	181	1630	20	3	6.7	< 3.5	282	190	2.1	1.01		
6	140	2040	6.7	4.8	14	8.4	199	132	1.2	2.8	246	132
7	235	1840	3	1.3	5.5	7.1	212	124	1.5	2.4	230	124
8	145	1820	20	1.3	22	7.4	220	162	1.2	1.07	930	162
9	155	1720	50	35	26	8.1	183	108	1.5		370	108
10	185	1970	4.2	1.3	11	8.6	329	88	1.4		355	88
11	144	1780	28	10	22	8.9	1231	196	1.7		635	196
12	165	1770	18	4.2	13	8.1	573	197	1.8		504	197
IEFD: 1.01 cm x 0.101 cm (0.04 in x 0.4 in) Area = 0.103 cm ²												
1	212	2090	47	46	56	3.5	141	103	1.7			
2	150	1610	20		5	4.9	142	117	1.2	2.0		
3	175	2080	34	39	52	5.9	67	51	1.09		514	42
4	124	1870	40	30	54	5.5	150	43	1.16			
5	158	1900	20	16	25	7.05	4035		Plat			
6	152	1900	23	22	27	5.0	259	202	1.3	7.1		
7	192	1860	44	41	49	6.0	317	260	1.17		194	252
8	144	1760	48	35	44	8.8	1126	895	1.87	1.51	524	868
9	134	1870	1.5	0.15	2.25	4.2	2287	1898	1.12		83	1840
IEPD: 1.90 cm x 0.202 cm (0.75 in x 0.08 in) Area = 0.386 cm ²												
1	190	1800	7.5	0.18	7.5	9.5	276	204	2.0	1.38	110	52
2	205	1800	93	71	93	9.2	2291	74	1.4	2.18	360	19
3	185	1720	16	5.5	9	17.6	5851	4228	Exp.	9.7	1500	324
4	195	1730	85	3.7	100	15	1807	1262	2.0	2.27	180	131
5	140	1690	34	2.1	17	9.9	926	512	1.3	1.32		
6	178	1710	77	1.4	40	17.1	1360	971	2.1		560	250

Table V (Continued)

IEPD Diameter: 0.89 cm (0.350 in) Area = 0.62 cm²

Tube Number	Cathode Sens. $\mu\text{a}/\text{W}$ 2870°K	Operating Voltage @2000a/1	Dark Current (amps x 10 ⁻¹⁰)		Equivalent Noise Input lumen x 10 ⁻¹⁴	Dark Pulses/Second		Peak-to-Valley Ratio	Noise Factor @200 a/1	Single Electron Pulses Per Second	
			@1800V	K@DZ @1800V		@80-90% C. Eff.	K@DZ*			Equivalent	Measured
1	170	1650	150	65	43	638		Plat.			
2	110	1600	68	41	18	870		Exp.			
3	100	1900	120		290	601		Exp.			
4	110	2280	0.2	0.1	23	290		Exp.			
5	98	1900	8.2	1.2	18	257		Plat.			
6	130	1750	14	11	7.8	393		Exp.			
7	155	1890	72	6.0	180	491		1.2		129 x 10 ¹	69 x 10 ¹
8	205	1770	32	1.5	25	917		1.4		250	127
9	175	2080	15		80	195		1.1		71	3
10	220	1850	70	0.9	94	4724		Plat.	2.46		
11	185	1850	80	16	110	9794		Exp.			
12	108	1900	27	24	50	2882		Exp.	1.75		
13	170	1800	53	0.42	53	471		1.2		266	6
14	160	1780	42	2.6	34	99		1.1		252	14
15	200	1800	75	0.6	75	827		1.2		740	104
Other IEPD											
1	215	1950	3.1	2.9	8	585		1.26		3540	1700
2	192	1640	48	4.6	18	1643		1.1		508	161
3	179	1760	33	1.9	24	201		1.9		2400	321
4	190	1860	24	2.2	33	957		Plat.			
5	211	1820	7.8	1.1	10	638		Exp.			
6	184	1920	7.3	6.8	8.3	80		1.4	6.5	38	38
7	158	1730	8	0.4	5	83		1.7		10300	2380
8	188		0.2	0.15	0.17	21		1.28		1980	< 800
Other IEPD											
			Tube Number		IEPD (CM)		IEPD AREA (CM ²)		IEPD (IN)		
			1		0.035 Diam.		0.001		0.014		
			2		0.76 x 0.24		0.193		0.3 x 0.1		
			3		0.071 x 0.71		0.0505		0.028 x 0.28		
			4		0.51 Diam.		0.202		0.20		
			5		0.51 Diam.		0.202		0.20		
			6		0.102 Diam.		0.081		0.04		
			7		0.0635 x 0.035		0.00225		0.025 x 0.014		
			8		0.0127 Diam.		0.000126		0.005		

For the purpose of a comparison between dark counts and dark current, an "observed single electron dark current", I_o , was defined at 1800 volts and extrapolated to 2000 amperes per lumen.

At 1800 volts:

$$I_o \text{ 1800 volts} = I_{\text{dark 1800 volts}} - I_{\text{dark K@D2}}$$

At 2000 amperes per lumen:

$$I_o \text{ 2000 a/l} = I_{\text{dark 2000 a/l}} \times I_o \text{ 1800 volts} / I_{\text{dark 1800 volts}}$$

The quantity $I_o \text{ 2000 a/l}$ is the dark current corrected for stem leakage and, perhaps, some multiplier contributions.

Next, a calculation was made of the dark pulse rate to which $I_o \text{ 2000 a/l}$ corresponds. Setting $I_o \text{ 2000 a/l}$ equal to I_o in the equation

$$N_o = I_o / e \mu_{dc}$$

where μ_{dc} is the d-c signal gain and

e is the charge of an electron

A prediction, N_o , was obtained of the number of single electron pulses per second which has occurred.

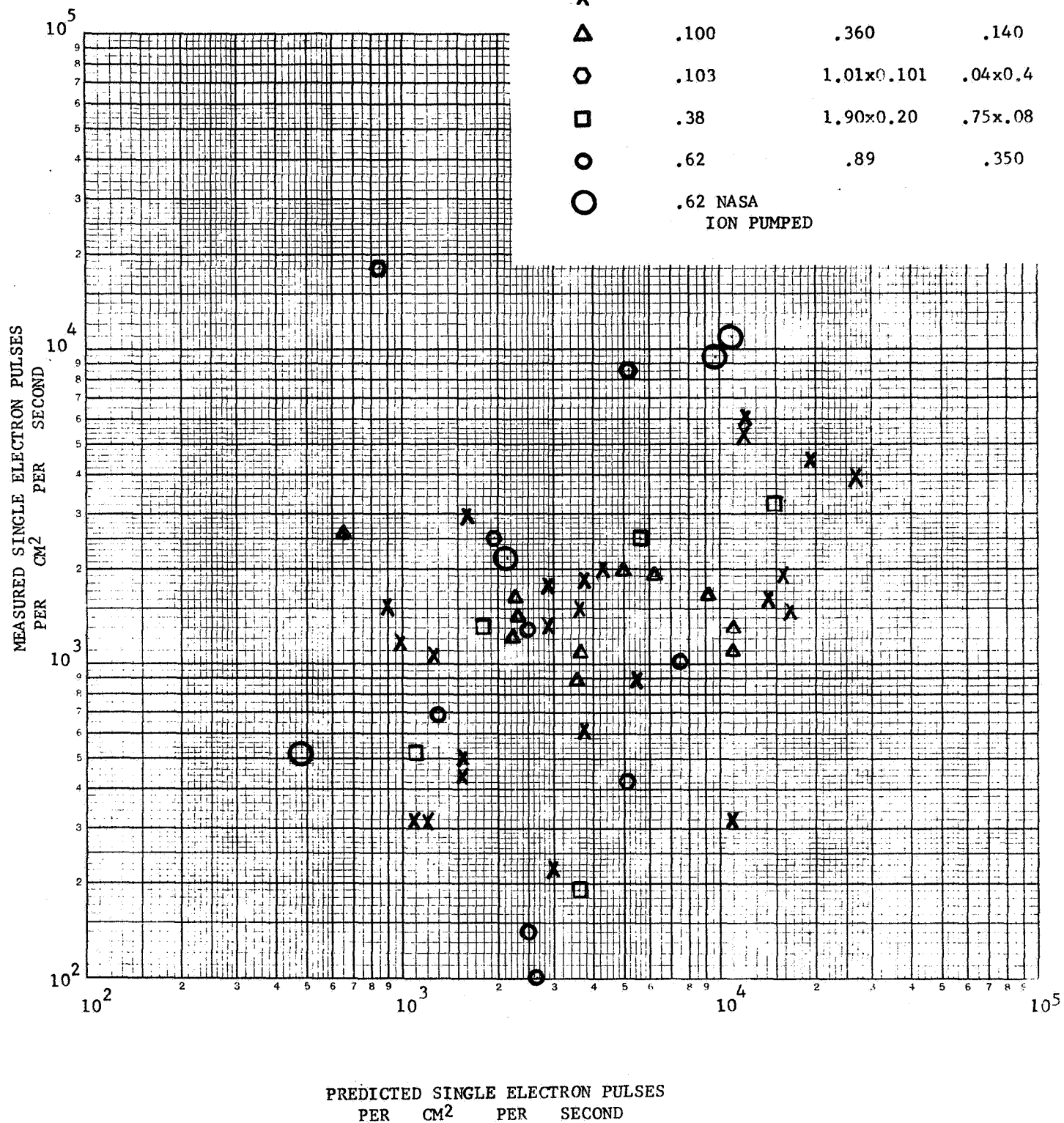
The measured (at 80 to 90 percent C. Eff. bias) anode pulses per second, N , and the predicted number, N_o , were normalized to the effective cathode area and plotted as the ordinate and abscissa respectively in Figure 38. The counting efficiency, always less than 100 percent, relates the expected values of N and N_o : $0.85 = N/N_o$.

A perfect correspondence between N and N_o would be observed in Figure 38 as all of the points lying on or near an "85 percent line."

- a. The predicted dark pulse rate, calculated from d-c parameters, is (on the average) greater than the actual, observed dark pulse rate. (Conversely, the d-c dark current is greater than the equivalent current resulting from single electron pulses.) The average order of magnitude of this effect is a factor of two.
- b. The ion-pumped tubes display a better absolute agreement between d-c predicted and the actual measured counting rates.

Figure 38

Symbol	Instantaneous Area (Cm ²)	Effective Photocathode Dimension (Cm)	(In)
X	.0506	.254	.100
△	.100	.360	.140
○	.103	1.01x0.101	.04x0.4
□	.38	1.90x0.20	.75x.08
○	.62	.89	.350
○	.62 NASA ION PUMPED		



- c. Better agreement for the other tubes might have resulted if d-c and pulse count measurements had been made nearly simultaneously; the discrepancy due to red sensitivity changes of the cathode and differences of temperature would have been eliminated. In addition, the use of pulse-count-optimized first and second dynode potentials in d-c measurements (rather than "standard potentials") would also reduce error.

In general, the predicted dark count, based on d-c dark current measurements, is greater than the measured dark count. This was expected, and it indicates that some anomalously large or small dark pulses are occurring. Large pulses due to cosmic rays¹¹ are to be expected, and small pulses due to such possibilities as dynode fluorescence, dynode bypassing, etc. are also to be expected. The contribution of these "spurious" dark pulses appears to be of approximately the same order of magnitude as the "true, single electron" dark counts.

It should be emphasized that dark leakage current (measured with the cathode at D2) has been subtracted from the dark current used to predict dark count in Figure 38. Examination of the data in Table V will allow a prediction of (greater) dark count if this dark leakage current is included.

The spread in the values of actual measured dark count (per unit area) in Figure 38 suggests one of two possibilities.

- a. Comparatively large experimental measurement errors.
- b. Comparatively large variations in cathode thermionic emission (including operating temperature changes).

Nevertheless it appears that the typical value of thermionic emission for S20 photocathodes, as formed in FW130 multiplier phototubes is:

$$1500 \begin{matrix} +1500 \\ -1100 \end{matrix} \text{ electrons/cm}^2/\text{sec}$$

Our specification of maximum permissible dark count of 100 c/sec for a 0.1 inch IEPD S20 photocathode (FW130 tube) may therefore be compared with an expected most probable value of $(1500)(0.05) = 75$ electrons/second.

11 A. T. Young, Rev. of Sci. Inst. 37,1472 (November 1966).

Cooled Data

Low temperature operation of multiplier phototube is necessary to acquire maximum information at low light levels and to separate and identify sources of dark pulses. For these reasons FW118 and FW130 cooled data from a production sampling of tubes (Tables VI and VII) was compiled. Typical values of the dark count at room temperature and at -70 degrees C are shown in Figure 39 with a simple extrapolation between. The FW130 exhibits a dark count reduction due to cooling of two to three orders of magnitude while the FW118 displays a reduction of about six orders. Measurements of count rates less than one per second were not made. The technique and the apparatus used for cooling the tube, especially the photocathode, and for measuring the dark pulses have been detailed elsewhere¹². Most pertinent is the fact that the phototube temperature was monitored by way of a thermocouple in contact with the faceplate. This arrangement facilitated accurate knowledge of cathode temperature only after thermal equilibrium had been reached.

12 Final Report NASw 1567, pages 20-25, 70 Nov. 16, 1966.

Cooled Characteristics

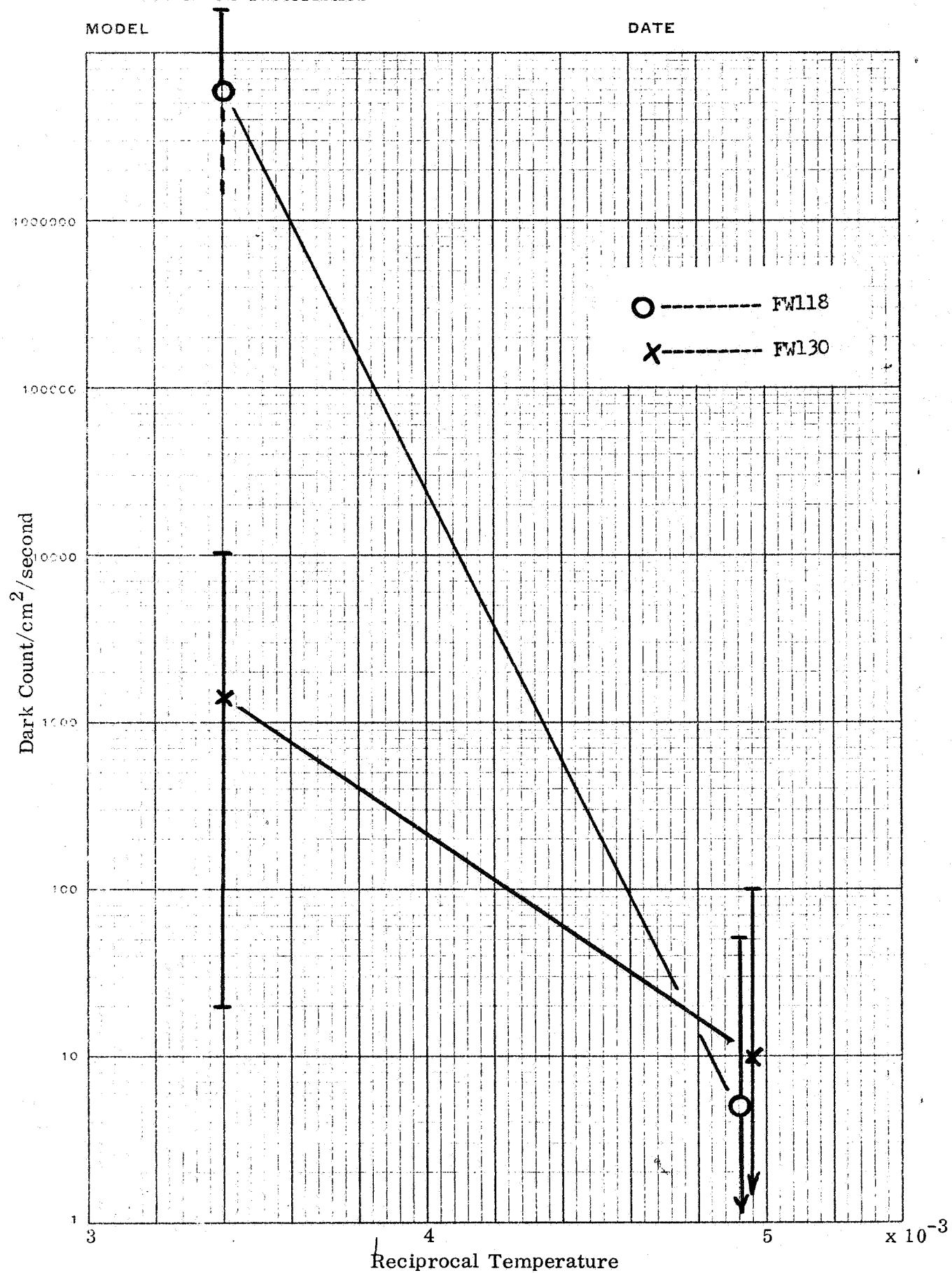


Figure 39

TABLE VI

FW - 118 Cooled Data

A Production Sample of Tubes

Tube Number	Temp. °C	IEPD Inches	Dark Pulses/Sec		Peak-to-Valley Ratio	Dark Current X10 ⁻¹⁰	Dark Pulse/cm ² /sec @80-90% C. Eff.
			Total Dark	@80-90% C. Eff. *			
1	-75	.100	123	4	1.6		80
2	-60		2	< 1	1.7		< 20
3	-70		6	< 1	1.4		< 20
4	-60		7	< 1	1.6	0.01	< 20
5	-60		3	< 1	1.4	0.003	< 20
6	-60		1325	11	1.16	0.008	218
7	-60		5	< 1	1.5	2.6	< 20
8	-80	.04x.40	23	< 1	1.6		< 10
9	-60	.350	11	2	1.3		3
10	-80		38	< 1	1.2		< 2
11	-67		10	3	1.3		5
12	-68		5	< 1	1.1		< 2
13	-60		519	42	1.2	0.1	67
14	-60		18	5	1.4	0.14	8
15	-60		7	5	1.5	440	8
16	-60		28	< 1	1.3		< 2
17	-60		92	66	1.5	0.1	105
18	-60		10	6	1.2		10
19	-60		2	< 1	1.3		< 2
20	-60		30	2	1.4	1.2	3
21	-65	.75x.08	54	< 1	1.7		< 3
22	-50		7	2	1.8		5
23	-64		1	< 1	2.2		< 3
24	-60		1	< 1	1.4		< 3

* Counting efficiency (See page 4-1).

TABLE VII

FW 130 Cooled Data

A Production Sampling of Tubes

Tube Number	Temp. °C	IEPD Inches	Dark Pulses/Sec Total Dark	Dark Pulses/Sec @80-90% C. Eff.	Total Cathode At D2	Peak-to Valley Ratio	Dark Current X10 ⁻¹⁵	Dark Pulses/cm ² /sec @80-90% C. Eff.
1	-60	.100	67	< 1	3	1.4	0.5	< 20
2	-70		294	11	15	1.1		218
3	-60		12	2		1.6	0.04	40
4	-60		74	2		1.5	0.05	40
5	-60		28	< 1	0	1.8		< 20
6	-60	.350	2	< 1		1.5	0.01	< 20
7	-60		1	< 1		1.3		< 20
8	-60		9	3		1.5		60
9	-70		171	48	10	1.5		78
10	-60		333	45		1.2	0.22	73
11	-60		30	10		1.1		16
12	-70		41	3		1.4		5
13	-70		95	17		1.1		27
14	-70		198	19	1	1.1		30
15	-70		17	5		1.1		8
16	-60		26	3	15	1.5	0.04	5
17	-70		7	< 1		1.4		< 2
18	-70		7	< 1		1.2		< 2
19	-70		27	20		1.2		32
20	-25		12	5		1.3	0.04	8
21	-60	.140	3	< 1		2.0		< 19
22	-70		3	< 1		1.4		< 10

TABLE VII (Cont.)

FW 130 Cooled Data

A Production Sampling of Tubes

Tube Number	Temp °C	IEPD Inches	Dark Total Dark	Dark Pulses/Sec @80-90% C. Eff.	Total Cathode At D2	Peak-to Valley Ratio	Dark Current X10 ⁻¹⁵	Dark Pulses/cm ² /sec @80-90% C. Eff.
23	-70		1	< 1	0	2.0	0.001	< 10
24	-60		2	< 1		1.9		< 10
25	-60		12	< 1	20	2.0		< 10
26	-60		22	5	0	2.0	0.4	50
27	-70	.200	2	2		1.1		10
28	-70	.200	3	< 1		1.2		< 5
29	-60	.40x.04	22	< 1	38	1.1		< 100
30	-25	.75x.08	860	143		1.2	0.4	370
31	-25		33	17	0	1.1		44
32	-25		66	36		1.9	0.11	93
33	-25		9	< 1		2.3		< 3
34	-25		3	< 1		1.4	0.01	< 3
35	-25		55	16		1.5	1.2	42
36	-25		260	31		1.2		80

7.0 CORRELATION OF DARK CURRENT AND DARK COUNTING RATE

Seven special tubes built on this contract were evaluated, both as to their d-c and photon counting characteristics in order to see if these could be correlated and to determine if the design innovation used held promise for improved performance.

The approach used was modifying the standard FW 130 phototube. The only non-standard feature of these tubes was a copper pumping tubulation connected to a one liter per second ion pump. This arrangement allowed evacuation to continue after a glass seal-off was made from the exhaust station. After removal from the exhaust station, the ion pump was started and allowed to operate until the pressure was of the order of 10^{-8} torr. At this time voltage was applied to the multiplier and the cathode was illuminated to produce an anode current of 200 microamperes. Drawing current from a multiplier always raises the gas pressure so it was hoped that this aging technique would produce a tube with lower residual gas pressure due to dynode outgassing. Pumping was continued in this manner until a pressure of the order of 10^{-9} torr was produced as indicated by the ion pump current. At this point the tube and the ion pump were separated by pinching the copper tubulation.

Measured and calculated characteristics of the seven tubes appear as Table VIII. It should be noted that the anode responsivity and the cathode sensitivity were the only two parameters that could not be measured directly in the pulse counting equipment. The same voltage divider was used in all measurements where a divider was required; and other changes of test equipment were avoided in order to eliminate possible error-producing variables.

Two dark current measurements were taken, one with the cathode at its normal high negative potential and the other with the cathode at dynode two potential. In the latter case all emission from the cathode was suppressed leaving only leakage to the anode pin and dynode dark emission as sources of dark current. If the equivalent dark currents are calculated for the measured dark counts with the cathode biased to dynode two potential, it is seen that agreement to the same order of magnitude is found (except for tube Nos. 106703 and 026831). This close agreement indicates that the anode guard ring in these tubes is quite effective in preventing anode pin leakage current from appearing in the output.

For the first four tubes, the data presented was taken at a constant gain of 5×10^6 . Gain is obtained by dividing the anode responsivity by the cathode sensitivity. The applicable cathode sensitivity is the larger of the two numbers in that column and is the response of the cathode to luminous flux from a tungsten lamp operated at a color temperature of 2870 degrees K; the second, and smaller, sensitivity value will be discussed in connection with data to be presented later in this section. The gain for these tubes was measured in both the dc and the pulse counting modes. The actual operating voltages were established on the basis of the constant d-c gain μ_{dc}

as mentioned earlier. The average gain (μ_{pc}) for the pulse counting mode was calculated for each tube by the relation

$$\mu_{pc} = \frac{Q}{e}$$

where $Q = C\bar{v}$, the product of C , the multiplier anode circuit capacity,

and \bar{v} is the average pulse amplitude of the single electron output pulses (obtained by examination of the pulse amplitude distribution).

The gain figures obtained by these two independent methods show fair agreement, though tube No. 106702 seems to differ rather widely even though a very good distribution was obtained, (as indicated by the good peak to valley ratio). Discrepancies between μ_{dc} and μ_{pc} would be more likely in the case of 106704 where the poor distribution would make it difficult to obtain the average pulse amplitude required for this calculation.

The rather large number of dark counts remaining at 80 to 90 percent counting efficiency is almost certainly due to the high red sensitivity of the photocathodes. This photocathode response is indicated by the smaller numbers in the cathode sensitivity column. They represent the response of the photocathode to 2870 degrees K luminous flux passed through a Corning 2418 glass filter, of half stock thickness, which transmits approximately 90 percent of all standard lamp radiation above 650 nm, to which the photocathode is sensitive.

For all tubes, the measured dc dark current may be converted into an equivalent dark count by using the d-c gain. (a second set of figures may be obtained by using μ_{pc} .) There is surprisingly close agreement between the calculated values and the actual numbers of dark counts at a counting efficiency of 80 to 90 percent. This fact may well be an indication that the dark counts removed by this calculated bias level are not tube contributed dark counts but rather preamplifier and external noise pickup. In any case it is an indication that low amplitude pulses do not affect the d-c measurements.

When cooled to -30 degrees C, four tubes showed dark counts of the order of 20 to 30 counts per second or less at 80 to 90 percent counting efficiency which indicates that dynode emission as well as cathode emission may be reduced to very low levels. Temperatures lower than -30 degrees C did not seem to produce lower dark counts; however, conclusive data is not available as the cooler is unable to maintain a temperature intermediate to room temperature and -60 degrees C long enough to assure that the cathode and the outer glass surface where the temperature is measured have come to equilibrium. A preliminary curve for the dark counts versus temperature is shown in Figure 37.

Data obtained for three tubes at -60 degrees C is displayed in Table IX. Pulse height spectra were determined at room temperature and -60 degrees C (Figures 40 and 41). The signal distributions, generally, are peaked at both temperatures. The occurrence rate of dark pulses of peak amplitude and larger amplitude is reduced from the room temperature level by an order of magnitude or more by operating at the low temperature.

A measure of the effect of using ion pumps while aging the FW130 phototubes might be attempted by calculating the departure of the parameters in Tables VIII and IX from those of a production sample (Tables V and VII). A simple comparison however shows that tube No. 026831 has an extraordinary cooled dark count and that the ion-pumped tubes are not otherwise different from the production sample either individually or as a group.

Table VIII

Tube Number	Cathode Sensitivity $\mu\text{a/L}$ *2870°K 2418 Filter	Anode Response Amperes/ Lumen	Divider Voltage	D. C. Gain (G) $\times 10^6$	Single Electron Pulse Gain (μ) $\times 10^6$	Dark Current $\times 10^{-10}$		Dark Counts Per Second * Equivalent Dark Current $\times 10^{-10}$			Calculated Dark Counts Per Second		Peak To Valley Ratio	ENI Lumens
						Total	Cath. at Dynode Two	Total	80 - 90% Counting Efficiency	Cath. at Dynode Two	Based On μpc	Based On μdc		
106701	*185 91	925	1790	5.0	4.22	36	0.11	*9753 67	*5900 40	*96 0.65	6000	4500	1.06	2.1
106702	*185 100	925	1760	5.0	3.48	1.9	0.16	*500 7.8	*330 1.8	*47 0.26	300	238	1.6	0.70
106703	*190 94	950	1970	5.0	4.96	52	7.2	*9839 78	*6250 49	*21 0.17	6540	6500	1.14	2.6
106704	*180 92	900	1880	5.0	5.62	12	0.16	*2010 18	*1330 12	*93 0.83	1330	1500	1.0	1.9
026817	*190 85	500	1900	2.6	**	26	0.10	328 13.7	300 12.5	4 .17		380	1.1	8.0
026825	*150 55	600	1800	4.0	**	2	0.12	189 12.1	151 9.7	1 .07		290	1.2	5.0
026831	*145 55	1500	2100	10.3	**	13	0.40	1408 23.2	1211 20.0	0.7 .01		870	1.1	7.2

** not determined

TABLE IX THREE FW130 PHOTOTUBES AT -60°C

Tube Number	Signal & Dark Current $\times 10^{-10}$	Signal & Dark Counts per Second		Dark Current $\times 10^{-10}$	Dark Counts per Second		Divider Voltage
		Measured at 80-90% C. Eff.	Calculated Based on D. C. Gain		Measured at 80-90% C. Eff.	Calculated Based on D. C. Gain	
026817	9.2	1454	2.2×10^3	.02	3	9	1900
026825	13	803	1.9×10^3	.03	3	4	1800
026831	12	2092	2.4×10^3	.45	129	91	1900

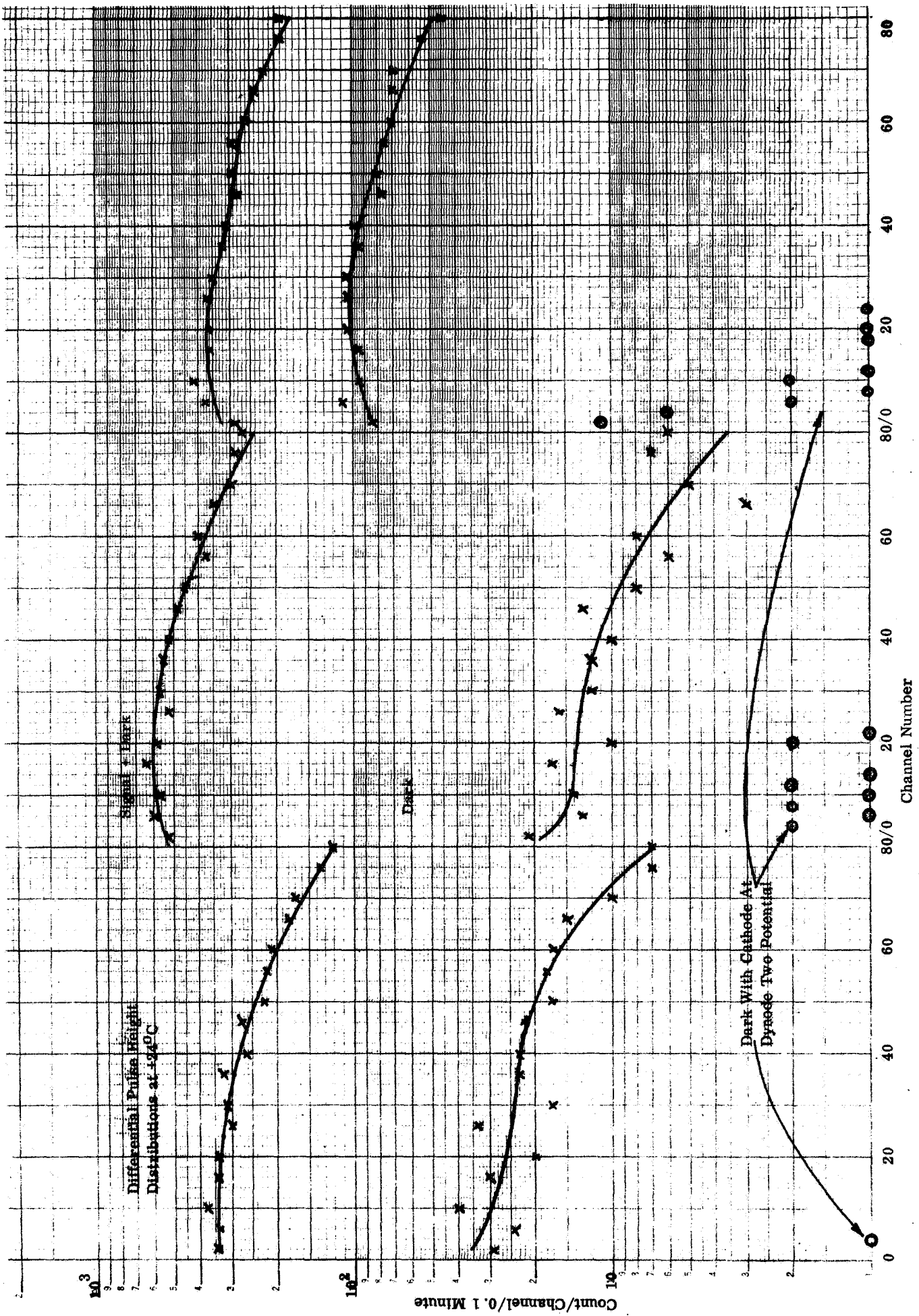


Figure 40

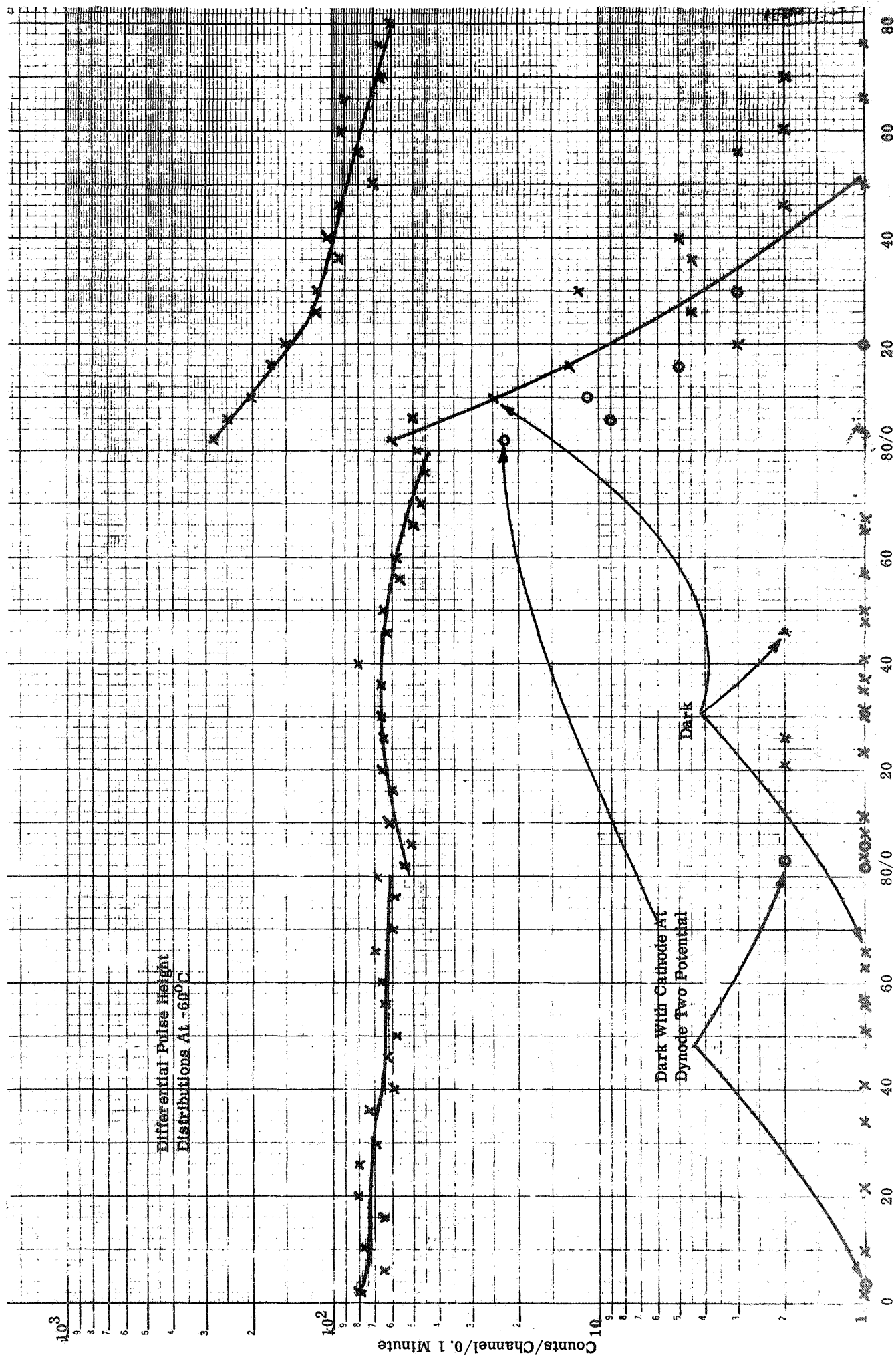


Figure 41